THE ASTROPHYSICAL JOURNAL, 353:494–523, 1990 April 20

GALACTIC BULGE M GIANTS. II. CONTENT AND STRUCTURE OF THE BULGE BETWEEN $b = -3°$ AND $-12°$

JAY A. FROGEL
Department of Astronomy, Ohio State University, and Kitt Peak National Observatory, National Optical Astronomy Observatories[1]
D. M. TERNDRUP AND V. M. BLANCO
Cerro Tololo Inter-American Observatory, National Optical Astronomy Observatories[1]
AND
A. E. WHITFORD[2]
Lick Observatory, Board of Studies in Astronomy and Astrophysics, University of California, Santa Cruz
Received 1989 June 9; accepted 1989 October 16

ABSTRACT

JHKL colors and CO and H_2O indices are presented for an unbiased sample of about 250 M giants drawn from complete surveys for such stars along the minor axis of the Galaxy at latitudes between $-3°$ and $-12°$. Magnitudes at 10 μm and narrow-band near-infrared colors for some of these stars are also given.

At constant $J-K$ the mean CO index of the bulge M giants weakens monotonically with increasing latitude. From the relation between CO and [Fe/H] established for star clusters, this would correspond to a decrease of $\sim$0.4 dex in the mean [Fe/H] between the $-3°$ and $-12°$ fields, from somewhat greater to somewhat less than solar. These values are consistent with abundances derived from optical color-magnitude diagrams. Despite these high [Fe/H] values, the ridgelines of the color-magnitude diagrams for all fields lie between those of 47 Tucanae and M3. There is a mild blueward shift with increasing latitude seen in the integrated mean $J-K$ colors of the fields.

A steady progression with latitude in the mean ($J-H$, $H-K$) relation for the bulge M giants is observed. For the $-12°$ field it is significantly displaced from the one for local field giants and overlaps that for globular cluster stars; for the $-3°$ field it is displaced by about the same amount, but on the opposite side of the field giant relation. Dispersions about this relation and the mean (CO, $J-K$) relation for the M giants in each field are comparable in size to the measuring uncertainties alone, but in a given field the *displacements* of individual stars from these two mean relations are statistically correlated. We attribute this correlation to a spread in metallicity within each field but note that this spread is smaller than the total metallicity range over all fields. In addition, metallicity-related effects result in $J-H$ getting *bluer* with increasing metallicity in stars of similar temperature.

The bolometric luminosity function of the nonvariable M giants is nearly independent of latitude. All show a sharp cutoff at $M_{bol} \leq -4.2$; such a cutoff could be a good extragalactic distance indicator for bulgelike stellar populations. The reddest ($J-K \geq 1.35$) and most luminous stars are found only in the low-latitude windows; all are M7–M9 giants, long-period variables (LPVs), or both. Except for these reddest stars, the ratio *at a given color* of M7–M9 giants to earlier type giants is independent of latitude. Only when stars of all colors in a spectral group are considered is the rapid falloff seen in the ratio of M7–M9 giants with respect to earlier types.

The bulge LPVs have $\langle M_{bol} \rangle = -4.2$. Since this is nearly the same as for LPVs in globular clusters, it does *not* require an age for the bulge population significantly younger than that of globular clusters. Their spatial distribution is similar to that of the reddest late M giants. The LPVs with the reddest colors, attributed to the most extensive circumstellar dust shells, are found in the lowest latitude fields. Most of the bulge *IRAS* sources in the fields studied can be identified with these LPVs or with the brightest nonvariable M giants; many of the latter are probably foreground objects. The reddest *IRAS* sources are at the lowest latitudes and have the coolest [12 – 25] μm colors. The bulge *IRAS* sources do not appear to represent a different or more luminous class of objects than the optically identified M giants.

Five different estimators of the surface brightness and surface density between latitudes $-3°$ and $-12°$ have a power-law dependence on radius with exponent between -2.5 and -3.4. The value of the exponent depends on the metallicity of the estimator: the most metal-rich objects have the steepest falloff. However, even the smallest exponent, which characterizes the *total* light and mass distribution, places the bulge among the most spatially concentrated of those measured by Kent for a sample of 22 Sb–Sc galaxies. Thus the mass distribution within the inner 1.5 kpc of the Galaxy is quite sharply peaked.

Subject headings: galaxies: stellar content — galaxies: The Galaxy — photometry — stars: abundances — stars: late-type — stars: long-period variables

[1] The National Optical Astronomy Observatories are operated by the Association of Universities for Research in Astronomy, Inc., under contract with the National Science Foundation.
[2] Visiting Astronomer, Cerro Tololo Inter-American Observatory.

I. INTRODUCTION

A study of stars in the bulge of the Milky Way is highly relevant for three important problems: the content and evolution of an old, metal-rich population; the evolution and chemical enrichment of the spheroidal component of the Galaxy; and the determination of the stellar content of typical E and S0 galaxies and the bulges of other spirals (Whitford 1978).

M giants are particularly numerous in the bulge; those in Baade's window at $l = +1°$, $b = -4°$ (Blanco, McCarthy, and Blanco 1984, hereafter BMB; Blanco 1986) have been the subject of recent detailed studies in the infrared by Frogel and Whitford (1987, hereafter FW) and in the optical by Rich (1988) and Terndrup (1988). These stars have different colors and luminosities from M giants in the solar neighborhood and from those used in stellar synthesis models, but have properties consistent with their being members of an old, metal rich population (cf. Frogel and Whitford 1982; Whitford 1985, 1986; Rich 1988). Differences between bulge and local giants are attributed to blanketing effects arising from the higher abundance of the bulge stars. FW demonstrated that the use of Baade's window M giants in stellar synthesis models results in close agreement between predicted and observed colors of early-type galaxies.

This paper extends FW's study to about 250 M giants in five other bulge fields between latitudes $-3°$ and $-12°$ along the Galaxy's minor axis. We set forth the evidence for radial gradients in the infrared colors, luminosities, and band indices of the M giants and offer an interpretation of these gradients in terms of an overall decrease in the metallicity at higher[3] latitudes in the bulge. We also establish the radial dependence of the integrated properties of the M giant population for their future use in stellar population models of external galaxies. The radial dependence of the surface density of the bulge as determined from the M giants is examined. There is a detailed discussion of long-period variables (LPVs) and bulge *IRAS* sources. Some of these new results have been outlined in Frogel (1988*a*, *b*). Analysis of 6000–9000 Å spectra of about 300 of the M giants in these five fields and in Baade's window and of 0.6–2.4 μm spectrophotometry of a subset of these stars will be presented in two subsequent papers (Terndrup, Frogel, and Whitford 1989 and Whitford, Terndrup, and Frogel 1990, hereafter Papers III and IV, respectively).

II. THE DATA BASE

a) Selection of Stars and Observational Techniques

i) *Spectral Classification and Photometry*

With a red grism at the prime focus of the CTIO 4 m telescope we searched for M giants in the Galactic bulge fields of daimeter 24'.4 that are listed in Table 1. Four overlapping fields were searched at $b = -12°$. The search technique was identical to that employed by BMB in Baade's window and is described fully by them (see also Blanco 1988; Blanco and Terndrup 1989). Some of the fields are well known: the Sgr I window near $b = -3°$, the area around the globular cluster NGC 6558 at $-6°$, and the field studied by van den Bergh and Herbst (1974) at $-8°$. The classification of the M giants proceeded somewhat differently from that in BMB. Rather than using all of the M subclasses, stars were placed in three bins: M2–M4, M5–M6, and M7 and later. For reasons discussed in Blanco (1986, 1987), incompleteness will be negligible except for the earliest M stars.

[3] Throughout this paper the terms "higher" and "lower" latitude will refer to greater and lesser distances from the Galactic plane, respectively, i.e., the sign of the latitude will be ignored.

TABLE 1

FIELDS SEARCHED FOR M GIANTS

Field	R.A.	Decl.	l	b	Notes
$-3°$.....	$17^h55^m.8$	$-29°15'$	1°.1	−2°.7	1
$-6°$.....	18 07.0	−31 46	0.2	−6.0	2
$-8°$.....	18 14.8	−32 53	0.0	−8.0	3
$-10°$.....	18 24.0	−33 58	359.9	−10.2	
$-10°$.....	18 25.5	−33 32	0.4	−10.3	
$-12°$.....	18 34.5	−34 43	0.5	−12.5	4

NOTES.—(1) Sgr I; (2) NGC 6558; (3) van den Bergh and Herbst 1974; (4) four areas.

Infrared observations with the CTIO 4 m reflector were obtained between 1983 and 1987 for a significant fraction of the M giants found in the fields in Table 1. These stars included nearly all classified as M7 or later and an unbiased selection from the M2–M4 and M5–M6 groups. Many of the stars that appeared to be particularly red in $H-K$ or have strong H_2O indices were also observed at L and at 10 μm. The equipment and observing techniques were the same as for the Baade's window observations (FW). Although there were several changes in detectors and Dewar optics during the course of this program, all data were transformed to the CTIO/CIT standard system (Elias *et al.* 1982). Repeated measurements of some of the stars in this program and in Baade's window demonstrated that the transformations, which in all cases were small, did not introduce any additional uncertainty to the photometry.

Tables 2–6 present the new reddening-corrected infrared data. Finding charts for these stars will be published separately (Blanco, Terndrup, and Frogel 1990). The second column indicates the spectral bin: 2 = M2–M4; 5 = M5–M6; and 7 = M7–M9. Reddening values for the fields at $-10°$ and $-12°$ were based on the maps of Burstein and Heiles (1982) and correspond to values of $E(B-V) = 0.18$ and 0.13, respectively, for an A0 star. For the $-8°$ window we used $E(B-V) = 0.25$ from van den Bergh and Herbst (1974); for the $-6°$ field we took the value $E(B-V) = 0.41$ from Zinn (1980) for NGC 6558. For the Sgr I field at $-3°$ we used $E(B-V) = 0.57$ for an A0 star. This value was derived by assuming that stars with the same TiO absorption strengths (measured by the reddening-free indices discussed in Paper III) at $b = -3°$ and $-3°.9$ will differ in observed $J-K$ color only because of reddening differences. Infrared and optical estimators of the metallicity gradient within the bulge indicate that the difference in TiO strength between these two fields due to the gradient will be small compared with the difference due to reddening. The extinction values used, derived with the reddening law in Cohen *et al.* (1981), are given in Tables 2–6 just below the observations of the bulge stars.

In some of the fields a number of the observed stars were judged to be foreground objects based on photometric criteria to be discussed below (§ II*a*[iii]). The data for these are given near the ends of Tables 2–6 below the extinction values and have *not* been reddening-corrected. If foreground stars were found among the stars identified in a grism plate, then the number of stars in that field in the relevant spectral group was reduced by a percentage equal to the number of foreground stars with infrared data divided by the *total* number of stars in that group with infrared data. These foreground dwarfs or

TABLE 2

REDDENING-CORRECTED PHOTOMETRY FOR M GIANTS AT $b = -3°$

Star	type	K	M_{bol}	J-K	H-K	K-L	H_2O	CO	102-C220	notes
3-01	2	9.78	-1.71	0.90	0.18		0.02	0.235		
3-03	5	9.45	-1.78	1.03	0.23		0.06	0.260	1.828	
3-12	2	9.44	-1.84	1.00	0.22		0.05	0.250		
3-13	7V	6.77	-4.21	1.33	0.55	0.62	0.65	0.170	2.166	
3-16	5	7.45	-3.56	1.28	0.38	0.23	0.37	0.310	2.518	
3-21	5	9.97	-1.59	0.87	0.15		0.03	0.210	1.511	
3-23	2	8.99	-2.50	0.90 3	0.15		0.02	0.190		
3-30	7V	6.78	-4.35	1.12	0.37	0.45	0.48	0.205	1.846	
3-31	5	8.90	-2.35	1.02	0.24		0.08	0.275	1.869	
3-33	2	8.64	-2.64	1.00	0.18		0.07	0.210	1.700	
3-35	7	8.26	-2.94	1.08	0.27	0.18	0.14	0.285	1.971	
3-39	7	8.30	-2.76	1.17	0.30	0.23	0.27 3	0.280	2.146	
3-46	5	8.38	-2.76	1.11	0.26		0.11	0.290		
3-48	2	10.60	-1.07	0.82	0.15		0.05	0.200		
3-52	5	8.46	-2.66	1.13	0.28	0.20	0.22	0.220	1.978	
3-60	2	7.84	-3.21	1.22	0.33	0.23	0.19	0.280	2.302	
3-64	5	8.34	-2.81	1.10	0.26		0.10	0.275	1.966	
3-68	2	10.35	-1.30	0.83	0.15		0.03	0.200	1.437	
3-75	5	9.65	-1.85	0.91	0.18		0.05 3	0.255		
3-80	5	8.62	-2.66	1.02	0.24		0.09	0.265		
3-84	5	8.40	-2.83	1.06	0.24		0.13 3	0.275		
3-86	2	10.66 6	-0.93	0.87 6	0.19 5		0.06	0.240		
3-92	5	9.03	-2.28	1.00	0.21		0.06	0.245		
3-99	2	10.72	-0.94	0.84	0.12		0.04	0.190		
3-109	5	8.84	-2.62	0.93	0.14		0.05	0.230 3		
3-113	5	7.87	-3.30	1.12	0.28		0.21 3	0.250		
3-118	5	10.24	-1.26	0.91	0.19		0.05	0.215		
3-123	2	9.04	-2.42	0.93	0.17		0.04	0.240		
3-127	7	7.52	-3.62	1.11	0.31	0.28	0.36	0.260	2.019	
3-128	5	7.34	-4.01	0.98	0.21		0.06 3	0.260		
3-133	5	10.59 5	-1.36	0.70 5	0.07 5		0.02	0.145		
extinction:		0.17		0.31	0.11	0.11	0.03	-0.02	0.55	
field stars:										
3-07	2	10.28		0.78	0.16		0.05	0.115		
3-40	2	12.63		0.28	0.09		0.02 3	0.000 3		
3-55	2	8.03		0.93	0.18					
3-74	2	11.62		0.32	0.06		0.03 3	-0.035 3	0.157	
3-93	2	10.68 6		0.81 6	0.17 5			0.080		
3-103	5	9.22		1.01	0.24 3		0.06	0.095		
3-106	2	12.10 3		0.35 3	0.05 2			0.040 4		
3-137	2	10.58 6		0.81 6	0.16 6		0.03 3	0.150 3		

giants will be ignored in the following analysis. In all cases. observational uncertainties are shown only if they are equal to or greater than 0.03 mag in $J-K$, $H-K$, or the molecular indices, 0.04 in $K-L$, and 0.06 in $K-[10]$.

ii) *Comments on the Individual Fields*

Because of the high stellar density in the $-3°$ window, only stars within a rectangular area 0.09 times that of a standard grism field were examined on the grism plate. Of these, 153 were classified as M giants of type M2 or later. The earlier M stars are often the most difficult to identify because of the weakness of their TiO bands, so it is possible that there is significant incompleteness in the list of identified early M giants. Of the 39 identified M stars for which infrared data were obtained and given in Table 2, seven of the M2–M4 stars and one M5–M6 star were judged to be foreground objects by the criteria set forth below.

At $b = -6°$ a full grism field was examined. The globular cluster NGC 6558 lies close to its middle. Of the 294 M giants found, 51 were observed in the infrared; the data are given in Table 3. None of these stars were considered foreground objects.

The $-8°$ field encompasses the areas studied by van den Bergh and Herbst (1974). Results of the grism survey have been presented by Blanco (1987). The 83 stars with infrared data given in Table 4 were drawn from a preliminary list of 150 M giants compiled by V. M. Blanco, whereas only 120 M giants are contained in this final list (Blanco 1987); stars earlier than M2 were rigorously excluded from his published list, whereas earlier M stars were included in the preliminary one. In order to maintain consistency with the other fields in the selection of M giants, we chose to work from the preliminary list. It so happens that none of the stars that Blanco had on his preliminary list but excluded from his published one were observed in

TABLE 3

REDDENING-CORRECTED PHOTOMETRY FOR M GIANTS AT $b = -6°$

Star	type	K	M_{bol}	J-K	H-K	K-L	H_2O	CO	K-[10]	102-C220	notes
6-3	5	8.17	-2.99	1.09	0.25		0.19	0.265			
6-6	2	9.52	-2.02	0.88	0.12		0.03	0.195			
6-7	5	8.49	-2.64	1.12	0.29		0.14	0.285			
6-9	5	8.91	-3.18	1.05	0.25		0.08	0.280			
6-12	5	8.12	-3.06	1.07	0.28		0.30	0.230			
6-16	2	9.18	-2.29	0.91	0.14		0.04	0.185			
6-19	5	8.03	-2.30	1.05	0.23		0.17	0.235			
6-21	2	10.15	-1.43	0.86	0.17		0.04	0.205			
6-23	5	6.66	-4.48	1.11	0.26		0.16	0.185			
6-28	2	8.04	-3.26	0.99	0.17		0.18	0.155			
6-29	5	7.93	-3.35	1.00	0.20		0.08	0.260			
6-34	2	10.50	-1.21	0.80	0.14		0.01	0.160			
6-37	5	9.97	-1.54	0.89	0.17		0.05	0.210			
6-39	2	8.88	-2.48	0.96	0.18		0.06	0.235			
6-43	7V	6.60	-4.46	1.19	0.44	0.57	0.55	0.120			
6-44	5	7.12	-4.01	1.12	0.28		0.18	0.280			
6-47	2	10.05	-1.51	0.87	0.16		0.05	0.215			
6-50	5	9.60	-1.83	0.93	0.19		0.06	0.200			
6-53	7V	7.31	-3.52	1.79	0.78	0.77	1.03	0.195	2.44 10		
6-55	2	10.17	-1.50	0.82	0.16		0.03	0.215			
6-58	5	7.36	-3.70	1.20	0.35		0.36	0.310		2.397	
6-60	7	6.86	-4.36	1.04	0.29	0.43	0.33	0.200			
6-61	2	9.25	-2.31	0.87	0.13		0.02	0.170		1.517	
6-67	2	9.83	-1.90	0.79	0.14		0.03	0.205			
6-69	5	7.85	-3.30	1.10	0.27		0.11	0.235		1.978	
6-74	2	9.53	-1.77	0.99	0.19		0.04	0.220		1.690	
6-75	5	10.63	-0.88	0.89	0.18		0.04	0.220			
6-80	5	9.86	-1.52	0.95	0.21		0.05	0.210		1.651	
6-82	5	7.50	-3.72	1.04	0.26		0.22	0.235		1.839	
6-83	2	9.49	-2.07	0.87	0.12		0.03	0.180		1.488	
6-85	5	10.46	-1.27	0.79	0.11		0.03	0.170		1.440	
6-88	5	8.04	-3.09	1.12	0.27		0.13	0.305		2.014	
6-91	5	8.96	-2.29	1.02	0.21		0.07	0.225		1.758	
6-93	5	7.22	-3.95	1.08	0.22		0.15	0.230		1.853	
6-95	5	7.83	-3.31	1.11	0.26		0.13	0.270		1.922	
6-97	2	10.19	-1.52	0.80	0.10		0.04	0.155			
6-99	5	7.43	-3.73	1.09	0.25		0.11	0.260		1.925	
6-104	2	9.71	-1.89	0.85	0.13		0.04	0.200			
6-109	7	8.48	-2.69	1.08	0.27		0.15	0.305			
6-114	7V	6.79	-4.31	1.15	0.42	0.43	0.73	0.245			
6-124	7	8.05	-3.04	1.16	0.33	0.25	0.32	0.285			
6-137	7	8.25	-2.77	1.26	0.38	0.33	0.29	0.280			
6-153	7	6.73	-4.28	1.27	0.38	0.28	0.40	0.310			
6-163	7V	6.56	-4.37	1.43	0.45	0.36	0.46	0.315			
6-169	7	7.43	-3.63	1.20	0.33		0.19	0.320			
6-170	7	7.46	-3.57	1.25	0.38		0.45	0.310			
6-171	7	8.38	-2.83	1.05	0.23		0.12	0.215			
6-199	7	8.57	-2.56	1.12	0.28		0.13	0.295			
6-212	7	6.87	-4.13	1.30	0.37	0.29	0.40	0.320			
6-227	7	8.13	-2.88	1.28	0.36		0.29	0.280			
6-235	7V	6.70	-4.09	2.39	1.06	1.22	1.05	0.095	3.93 10		IRAS
extinction:		0.12		0.22	0.08	0.08	0.02	-0.015	0.12	0.380	

the infrared. All of Plaut's (1971) M and SRa variables in the $-8°$ grism field were selected as M giants by Blanco. Numbers assigned by Plaut and by Blanco (1987) are given in the Notes column of Table 4. Four of the stars in Table 4 can be identified with *IRAS* sources. None of the stars in Table 4 appeared to be foreground objects.

At $-10°$ the surface density of stars has declined markedly from that at lower latitudes. Thus two entire grism fields were scanned for M stars; 101 were found, 45 of which were observed in the infrared; the data are in Table 5. Eight of the 45 were found to be field M (or late K) dwarfs from their colors, indices, and/or CCD spectroscopy. Thus, the adjusted number of M giants is 86, of which 37 have infrared data. Data were also obtained for V1889 Sgr, a Mira variable just outside of the grism field.

At $-12°$ four overlapping grism fields were scanned for M stars. The total effective area was equal to 3.57 standard grism fields. Of the 144 stars tentatively identified as M giants, 52

TABLE 4

REDDENING-CORRECTED PHOTOMETRY FOR M GIANTS AT $b = -8°$

Star	type	K	M_{bol}	J-K	H-K	K-L	H_2O	CO	K-[10]	notes
8-1	2	7.88	-3.55	0.93	0.18		0.04	0.215		106
8-4	7	8.19	-2.85	1.17	0.32	0.26	0.23 3	0.290		100
8-6	5	7.73	-3.41	1.11	0.30	0.27	0.19 3	0.310		105
8-7	2	10.04	-1.48	0.89	0.17		0.03	0.215		116
8-8	5	9.39	-1.99	0.95 3	0.20		0.04	0.225		117
8-9	5	7.70	-3.44	1.11	0.28	0.25	0.14 3	0.215		118
8-12	5	8.38	-2.90	1.00	0.19	0.23 4	0.09	0.225		109
8-14	7	7.15	-3.85	1.29	0.38	0.35	0.30 3	0.310		99
"	"	7.16		1.29	0.37	0.30	0.29	0.300	1.30 8	
8-15	2	9.84	-1.50	0.97	0.21		0.03	0.185		101
8-19	5	8.78	-2.54	0.98	0.22		0.03	0.255		112
8-21	2	10.34	-1.22	0.87	0.15		0.00	0.175		104
8-23	5	9.09	-2.25	0.97	0.20		0.03	0.235		91
8-24	2	11.21		0.47	0.07		-0.00	0.070		87
8-25	2	9.53	-1.96	0.90	0.19		0.03	0.210		92
8-26	2	8.84	-2.54	0.95	0.21		0.03	0.250		96
8-29	7V	6.75	-4.39	1.11	0.38	0.56	0.48 3	0.190		IRAS
"	"	7.58		1.22	0.52	0.53	0.99	0.185	1.94 8	P456
8-31	2	9.84	-2.04	0.72	0.10		0.00	0.085		90
8-32	5	7.97	-3.28	1.02	0.22		0.04	0.235		94
8-33	7	7.83	-3.31	1.11	0.31	0.31	0.27 3	0.275		85
8-34	5V	7.48	-3.70	1.07	0.39	0.61	0.58 3	0.280		P446
"	"	7.16		0.97	0.27	0.43	0.31	0.310	1.37 8	86
8-35	2	9.42	-1.81	1.03	0.24		0.07	0.255		78
8-38	2	7.25	-4.13	0.95	0.19	0.17 4	0.05	0.235		77
8-40	5	8.54	-2.68	1.04	0.25		0.06	0.235		82
8-43	7V	5.03	-6.06	1.16	0.41	0.53	0.44	0.210		IRAS
"	"	5.83		1.31	0.55	0.56	0.97	0.255	1.81	P434
8-44	5	9.47	-1.73	1.06	0.23		0.09	0.220		
8-45	2	9.58	-1.89	0.91	0.16		0.02	0.225		71
8-49	2	11.36		0.45	0.07		0.00	0.065		
8-51	5	9.36	-1.84	1.06	0.23		0.28 3	0.220		72
8-54	2	10.56	-1.34	0.71	0.10		0.02	0.130		
8-56	5	7.74	-3.40	1.11	0.29	0.26	0.10	0.285		43
8-57	5	10.44	-0.94	0.95	0.16		0.10 3	0.195		
8-59	5	8.70	-2.46	1.09	0.28		0.10	0.275		55
8-61	5	10.12	-1.35	0.91	0.20		0.01	0.180		64
8-62	5	9.02	-2.24	1.01	0.23		0.05	0.250		57
8-63	2	10.03	-1.49	0.89	0.15		0.03	0.180		
8-65	5	8.43	-2.79	1.04	0.22		0.06	0.225		56
8-69	5	9.82	-1.61	0.93	0.21		0.03	0.220		59
8-71	5	7.96	-3.24	1.06	0.25		0.06	0.220		63
8-72	5	8.34	-2.94	1.00	0.22		0.06	0.220		61
8-73	2	10.47	-1.16	0.84	0.16		0.02	0.200		
8-75	7	7.68	-3.42	1.15	0.31	0.22 4	0.13	0.280		50
8-76	5	9.26	-2.08	0.97	0.20		0.03	0.225		44
8-77	5	7.04	-4.17	1.05	0.25	0.19 4	0.17	0.255		46
8-78	5	9.84	-1.46	0.99	0.23		0.04	0.245		
8-81	7V	6.85	-4.18	1.25	0.43	0.47 4	0.56	0.280		IRAS
"	"	6.83		1.30	0.44	0.42	0.52	0.285	1.46 6	39
8-82	5	8.59	-2.63	1.04	0.21		0.12	0.220		33
8-84	5	8.45	-2.85	0.99	0.23		0.03	0.230		35
8-85	2	8.41	-2.93	0.97	0.20		0.04	0.260		37
8-86	7V	6.00	-5.05	1.22	0.48	0.66 4	0.60	0.165		41,IRAS
"	"	5.80		1.17	0.39	0.55	0.42	0.250	1.80	P385
8-88	5	5.69	-5.56	1.02	0.26	0.26	0.24	0.230		31
8-90	5	9.28	-2.10	0.95	0.21		0.01	0.190		32
8-91	5	10.09	-1.27	0.96	0.22		0.00	0.190		36
8-93	7	8.80	-2.33	1.12	0.29		0.08	0.275		23
8-94	2	10.59	-1.12	0.80	0.13		0.01	0.195		
8-96	7V	7.12	-3.88	1.30	0.56	0.58	0.98 3	0.250		P363
"	"	6.99		1.19	0.45	0.59	0.60	0.180	1.05 8	20
8-97	5	9.11	-2.12	1.03	0.22		0.03	0.210		18
8-98A	5	9.50	-1.82	0.98	0.23		0.04	0.220		9
8-99	2	10.01	-1.40	0.94	0.22		-0.00	0.210		2

TABLE 4—*Continued*

Star	type	K	M_{bol}	J-K	H-K	K-L	H_2O	CO	K-[10]	notes
8-100	5	8.28	-2.93	1.05	0.24		0.02	0.220		8
8-102	5	9.78	-1.45	1.03	0.20		0.08	0.225		25
8-105	5	8.12	-3.02	1.11	0.31		0.09	0.270		12
8-106	2	10.02	-1.63	0.83	0.15		0.06	0.170		4
8-109	5	7.96	-3.38	0.97	0.19		0.02	0.195		
8-110	4V	8.16	-2.96	1.13	0.42	0.57	0.89	0.245		P328
8-111	5	8.40	-2.88	1.00	0.21		0.09	0.200		21
8-112	2	9.22	-2.10	0.98	0.23	0.13 4	0.05	0.215		
8-114	5	8.27	-3.01	1.00	0.18		0.07	0.215		7
8-116	7	7.43	-3.70	1.12	0.30	0.36 4	0.17	0.190		17
8-117	5	8.02	-3.19	1.05	0.23		0.05	0.245		27
8-119	7	6.98	-3.97	1.37	0.43	0.37	0.41	0.330		24
"	"	6.80		1.34	0.39	0.33	0.29	0.285	1.24 9	
8-120	2	8.90	-2.42	0.98	0.20		0.05	0.235		
8-121	5	9.09	-2.16	1.02	0.20		0.05	0.220		119
8-122	5	8.03	-3.42	0.92	0.17		0.05	0.210		108
8-123	7	8.20	-3.01	1.05	0.24		0.09	0.175		102
8-124	2	9.36	-2.27	0.84	0.12		0.05	0.175		
8-127	5	9.91	-1.52	0.93	0.19		0.05	0.235		73
8-129	2	9.60	-1.96	0.87	0.21		0.03	0.195		53
8-133	2	10.18	-1.34	0.89	0.14		0.04	0.205		49
8-137	2	10.07	-1.40	0.91	0.14		0.04	0.160		66
8-141	2	9.93	-1.63	0.87	0.18		0.03	0.220		
8-145	2	9.69	-1.76	0.92	0.14		0.05	0.190		14
8-149	2	8.72	-2.58	0.99	0.21		0.07	0.240		13
8-153	2	9.65	-1.87	0.89	0.14		0.04	0.195		
extinction:		0.07		0.14	0.05	0.05	0.02	-0.01 0.07	0.24	

were observed in the infrared; the data are in Table 6. Eight of the 52 have colors typical of foreground dwarfs or early-type stars. The adjusted number of M giants is then 127, of which 44 have infrared data. Two suspected LPVs, Nos. 17 and 56, were observed twice, about a year apart. There are two possible identifications with *IRAS* sources.

iii) *Field Stars*

A few obvious foreground stars —mostly late K or M dwarfs but also some early-type stars of unknown intrinsic luminosity—were found in the $-3°$, $-10°$, and $-12°$ fields. In nearly all cases the classification was clear cut: their $J-H$, $H-K$ colors and, when available, their CO and H_2O indices lay on or close to the mean relations for dwarfs (Frogel *et al.* 1978, hereafter FPAM; Aaronson, Frogel, and Persson 1978). CCD spectra (Paper III) of most of these stars displayed the strong infrared Na doublet characteristic of dwarfs. Figures presented later in this paper will illustrate the ease of picking out dwarfs. Although some LPVs can have $J-H$, $H-K$ colors similar to those of dwarfs, their CO and H_2O indices are quite different, as are their luminosities and CCD spectra; LPVs are amongst the brightest stars in a field, whereas the identified dwarfs are invariably among the faintest. A few stars, mostly in the $-3°$ window, were judged to be early-type foreground objects because of their overall blueness and weak band indices. Again, CCD spectroscopy, when available, confirmed such an identification from an obviously discrepant radial velocity. All of the data for the identified foreground stars are given at the end of the appropriate table for each field. These data have *not* had any reddening corrections applied. Finally, we note that some fraction of the M giants (10%–20% according to Blanco and Terndrup 1989) could be disk objects. Although they would be expected to have relatively bright M_{bol}, we are not presently able to specify which of the stars in Tables 2–6 they are.

b) Bolometric Magnitudes

Bolometric magnitudes for stars in the $-3°$, $-6°$, and $-8°$ windows were calculated from their $(J-K)_0$ colors and the mean relation between this color and BC_K determined from observations of M giants in Baade's window (Fig. 1*b* of FW). As we will show later in the paper, M giants in the $-10°$ and $-12°$ windows have *JHK* colors more similar to those of local field giants than Baade's window giants, so bolometric corrections for them were determined from the mean relation for field giants (Fig. 1*b* of FW) based on the mean colors given in FPAM. The resulting bolometric magnitudes are given in Tables 2–6. For consistency, we assume a distance to the bulge of 7 kpc, the value used in FW. This is somewhat less than Reid's (1989) best-value estimate of 7.7 ± 0.7 kpc that includes the most recent radio proper-motion data. Adoption of Reid's value would make all luminosities brighter by 0.2 mag and would increase linear scales by 10%. While this change would in no way alter the conclusions of this paper, its effect on the results has been noted where appropriate.

III. LATITUDE DEPENDENCE OF THE COLORS, MAGNITUDES, AND INDICES

The *JHK* colors and CO and H_2O indices of M giants in Baade's window differ markedly from those of giants in the solar neighborhood and in globular clusters (FW). In this section we will set forth the relations between these colors and indices for stars in all of the bulge fields and consider the

TABLE 5

REDDENING-CORRECTED PHOTOMETRY FOR M GIANTS AT $b = -10°$

Star	type	K	M_{bol}	J-K	H-K	K-L	H_2O	CO	K-[10]
10-01	2	9.19	-2.26	0.99	0.19		0.05	0.210	
10-03	5	9.59	-1.94	0.96	0.20		0.04	0.200	
10-04	2	10.58	-1.07	0.90 3	0.16		0.05 3	0.190	
10-06	5	10.00	-1.43	1.00	0.22		0.05	0.230	
10-07	2	8.89	-2.54	1.00	0.19	0.17	0.06	0.200	
10-09	2	8.93	-2.52	0.99	0.21	0.21	0.23	0.250	
10-10	7	7.11	-4.08	1.16	0.32	0.28	0.40	0.280	
10-12	2	9.66	-1.94	0.93	0.19		0.04	0.180	
10-14	7	7.71	-3.57	1.09	0.26	0.22	0.08	0.260	
10-15	2	10.02	-1.63	0.90	0.19		0.04	0.210	
10-17	2	10.35	-1.38	0.86	0.18		0.04	0.190	
10-18	5	9.86	-1.72	0.94	0.21		0.04	0.210	
10-22	2	11.17	-0.66	0.79	0.14		0.04 3	0.150	
10-23	2	9.83	-1.85	0.88	0.14		0.03	0.155	
10-24	2	10.32	-1.31	0.91	0.19		0.07 3	0.210	
10-25	2	10.65	-1.23	0.76	0.10		0.03	0.140	
10-26	2	10.77	-1.17	0.73 3	0.10		0.03 3	0.105	
10-27	5	11.03	-0.76	0.82	0.13		0.02	0.170	
10-28	5	9.42	-2.11	0.96	0.20		0.06	0.210	
10-30	2	8.85	-2.98	0.79	0.12		0.03	0.165	
10-33	2	7.29	-4.24	0.96	0.16	0.15	0.05	0.200	
10-37	2	10.78	-0.95	0.85	0.13		0.02	0.160	
10-40	2	10.40	-1.27	0.89	0.17		0.03	0.205	
10-42	5	7.41	-3.93	1.05	0.24	0.15	0.10	0.240	
10-43	5	10.80	-0.70	0.97	0.19		0.04	0.200	
10-45	2	9.09	-2.52	0.92	0.15		0.04	0.160	
10-46	7	9.37	-2.13	0.97	0.21		0.05	0.215	
10-48	2	10.82	-0.83	0.90	0.18		0.04	0.205	
10-50	5	7.94	-3.35	1.08	0.23	0.15	0.09	0.220	
10-51	2	10.20	-1.63	0.79	0.11		0.04	0.115	
10-52	5	8.70	-2.63	1.06	0.26		0.07	0.255	
10-53	5	9.32	-2.06	1.03	0.21	0.11	0.05	0.210	
10-55	7	7.27	-3.88	1.19	0.33	0.30	0.27	0.235	
10-57	5	6.38	-4.95	1.06	0.22	0.18	0.08	0.245	
10-100	5	8.14	-3.20	1.05	0.22		0.08 3	0.215	
10-101	5	8.99	-2.29	1.09	0.27		0.08 3	0.235	
10-101A	C	8.80	-2.73	0.96	0.23		0.08 3	0.155	
10-102	5	8.12	-3.02	1.20	0.36		0.27 3	0.330	
10-1889	5V	8.29	-3.36	0.90	0.32	0.50	0.58	0.190	
extinction:		0.05		0.10	0.03	0.03	0.01	-0.005	
field stars:									
10-20	5	11.66		0.83	0.21		0.14	0.030	
10-21	2	11.41		0.78	0.14		0.07	0.040	
10-29	5	11.95		0.87	0.27		0.22	0.000	
10-32	5	12.60		0.86	0.19				
10-35	2	10.09		0.66	0.11		0.04	0.080	
10-39	5	11.86		0.86	0.23		0.17	0.010	
10-44	5	12.06		0.89	0.24		0.13	0.010	
10-54	7	11.37		0.88	0.31		0.31	0.000	

implications for the derivation of the metallicity of bulge giants both within a given field and as a function of latitude.

a) Mean and Median Colors and Magnitudes

Flux-weighted means and medians of the magnitudes, colors, and indices for each of the three spectral groups of M giants in each of the bulge fields were calculated by weighting the contribution of each star at a given wavelength by its luminosity at that wavelength. These weighted mean colors are approximations to those that would actually be observed in isolated samples of such stars. The values are given in Table 7. At the bottom of the entries for each field are the number of giants in each class identified in the grism surveys, adjusted for the number of identified interlopers as described earlier, and the number in each class with infrared data given in Tables 2–6.

Inspection of Table 7 shows that the *particular* spectral groups have colors and indices that are basically independent of latitude. They are not noticeably affected by the metallicity gradient in the bulge (redder colors for the M1–M4 stars in the

TABLE 6

REDDENING-CORRECTED PHOTOMETRY FOR M GIANTS AT $b = -12°$

Star	type	K	M_{bol}	J-K	H-K	K-L	H_2O	CO	102-C220	notes
12-01	5	5.87	-5.27	1.21	0.31	0.26	0.29	0.280	2.22	IRAS
12-04	2	10.52	-1.34	0.77	0.09		0.03 3	0.115 2		
12-06	2	10.14	-1.67	0.81	0.10		0.03 3	0.165		
12-08	5	7.54	-3.67	1.14	0.26	0.22 4	0.19	0.250	1.99	
12-09	7	7.15	-4.04	1.16	0.27		0.14	0.275	1.96	
12-10	2	8.91	-2.70	0.92	0.14		0.04 3	0.185		
12-11	5	8.66	-2.72	1.02	0.19		0.10	0.225	1.73	
12-13	2	9.31 4	-2.19	0.97 4	0.15 3		0.12 3	0.255		
12-15	2	9.48	-2.19	0.89 3	0.12		0.03 3	0.180		
12-16	5	7.23	-4.20	1.00	0.16		0.09	0.200	1.67	
12-17	7V	6.36	-4.79	1.19	0.46	0.68	0.50	0.190	1.91	IRAS
"	"	6.49		1.49	0.62		0.77 3	0.245		
12-19	2	7.76	-3.69	0.99	0.19		0.05 3	0.225		
12-21	2	9.34	-2.21	0.95	0.16		0.05 3	0.205		
12-23	2	9.92	-1.89	0.81	0.11		0.03 3	0.175		
12-25	2	9.24	-2.36	0.93	0.14		0.04 3	0.185		
12-27	5	7.81	-3.52	1.05	0.21		0.10	0.250	1.78	
12-28	2	11.02	-0.98	0.70 3	0.09		0.04 3	0.095		
12-33	5	9.32	-1.94	1.10	0.21		0.17	0.220	1.84	
12-36	2	9.55	-2.41	0.72	0.10		0.06 3	0.135		
12-38	2	10.39	-2.00	0.50	0.06			0.065		
12-39	2	10.76	-1.34	0.65	0.11		0.06 3	0.040		
12-40	2	10.10	-1.50	0.93	0.13		0.05 3	0.185		
12-41	2	10.29	-1.88	0.61 3	0.09		0.03 3	0.110		
12-42	2	6.34	-5.24	0.94	0.15		0.06 3	0.200		
12-43	2	5.89	-5.79	0.88	0.15		0.05 3	0.185		
12-44	5	11.22 7	-0.72	0.73 5	0.09 5		0.06 3	0.140		
12-45	2	10.57 3	-1.63	0.60 3	0.07		0.04 3	0.080		
12-46	5	10.53 3	-1.29	0.80 3	0.09		0.05 3	0.145		
12-48	2	10.57 3	-1.33	0.75 3	0.11		0.05 3	0.150		
12-50	2	10.28 4	-1.39	0.89 3	0.15 3		0.07 2	0.180		
12-54	2	11.09	-0.93	0.69 2	0.09		0.03 2	0.090 2		
12-55	5	9.99	-1.68	0.89	0.12			0.150	1.49	
12-56	7V	7.98	-3.16	1.26	0.53	0.64 4	0.84	0.135	2.09	
"	"	7.90		1.13	0.45		1.23 2	0.315		
12-57N	?	11.37 4		0.69 2	0.08			0.085		
12-58	5	10.76	-0.92	0.88	0.13		0.03 2	0.165		
12-59	5	8.41	-2.95	1.03	0.21		0.08 2	0.225		
12-60	5	8.96 3	-2.62	0.94 3	0.16		0.04 2	0.180		
12-62	5	6.56 3	-5.02	0.94 3	0.20		0.04 2	0.240		
12-63	5	7.63 3	-3.75	1.02 3	0.21		0.06 2	0.210		
12-64	5	8.13 3	-3.20	1.05 3	0.23		0.16 3	0.240		
12-65	5	7.40 3	-3.83	1.13 3	0.29		0.16 2	0.255		
12-66	5	7.77 3	-3.56	1.06 3	0.23		0.13 2	0.215		
12-67	5	7.66 3	-3.60	1.10 3	0.26		0.23 2	0.245		
12-68	5	7.72 3	-3.56	1.09 3	0.26		0.09 2	0.300		
12-69	5	5.52 3	-5.72	1.12 3	0.27	0.20 3	0.13 2	0.240		
extinction:		0.04		0.07	0.03	0.03	0.01	-0.005	0.13	
field stars:										
12-30	2	12.73 2		0.42 3	0.02					
12-35	7	12.51 2		0.77 2	0.12					
12-37	2	11.68		0.34 2	0.05					
12-51	5	12.49 4		0.84 3	0.26 3		0.19 3	-0.030 3		
12-57	7	11.88		0.21	-0.03			0.000		
12-61	5	11.67 3		0.85 3	0.34 2					
12-70	7	9.69 3		0.95 3	0.35	0.41 8	0.26 2	-0.060		
12-71	5	11.32 3		0.83 3	0.29		0.27 3	-0.020		

TABLE 7

REDDENING-CORRECTED MEAN AND MEDIAN COLORS AND MAGNITUDES FOR FIELDS IN THE GALACTIC BULGE

	Means			Medians		
	M1-4	M5-6	M7+	M1-4	M5-6	M7+
−12° Window						
K	8.30	7.38	6.97	10.10	7.81	7.15
J-K	0.90	1.09	1.19	0.81	1.04	1.19
H-K	0.15	0.25	0.41	0.11	0.21	0.46
K-L	...	...	...	...	...	...
H_2O	0.05	0.145	0.44	0.05	0.095	0.495
CO	0.19	0.245	0.21	0.175	0.225	0.19
No. of stars	100	24	3			
No. with IR	21	20	3			
−10° Window						
K	9.36	8.25	7.59	10.20	8.99	7.49
J-K	0.92	1.05	1.14	0.90	1.03	1.13
H-K	0.16	0.24	0.30	0.16	0.22	0.29
K-L	...	...	...	...	...	0.25
H_2O	0.06	0.125	0.265	0.04	0.07	0.18
CO	0.19	0.24	0.255	0.19	0.215	0.25
No. of stars	58	24	4			
No. with IR	19	15	4			
−8° Window						
K	9.19	8.18	6.75	9.76	8.57	7.15
J-K	0.94	1.03	1.19	0.90	1.02	1.16
H-K	0.20	0.25	0.41	0.17	0.22	0.38
K-L	...	...	0.50	...	...	0.36
H_2O	0.12	0.15	0.46	0.035	0.055	0.305
CO	0.22	0.235	0.225	0.20	0.225	0.275
No. of stars	96	41	13			
No. with IR	30	40	13			
−6° Window						
K	9.40	7.94	7.23	9.62	8.04	7.37
J-K	0.91	1.09	1.32	0.87	1.07	1.22
H-K	0.15	0.26	0.45	0.14	0.25	0.37
K-L	...	...	...	...	...	0.29
H_2O	0.075	0.17	0.52	0.04	0.13	0.37
CO	0.19	0.245	0.24	0.195	0.235	0.28
No. of stars	173	104	17			
No. with IR	14	21	16			
−3° Window						
K	9.19	8.50	7.33	9.61	8.73	7.52
J-K	1.02	1.07	1.19	0.90	1.02	1.12
H-K	0.23	0.24	0.40	0.18	0.24	0.31
K-L	...	...	0.45	...	...	0.28
H_2O	0.095	0.15	0.47	0.05	0.07	0.36
CO	0.24	0.24	0.215	0.22	0.26	0.26
No. of stars	41	73	5			
No. with IR	10	16	5			

TABLE 8

REDDENING-CORRECTED, NORMALIZED MEAN COLORS AND INTEGRATED MAGNITUDES FOR M GIANTS IN BULGE FIELDS

	Field					
Characteristic	−3°	−4°	−6°	−8°	−10°	−12°
Size	0.09	1.00	1.00	1.00	2.00	3.57
K	0.79	1.03	2.29	2.92	4.71	4.13
$J-K$	1.07	1.05	1.08	1.06	0.99	0.97
$H-K$	0.26	0.28	0.26	0.29	0.22	0.20
H_2O	0.18	0.21	0.21	0.26	0.12	0.10
CO	0.24	0.24	0.23	0.23	0.22	0.21

−3° field arise from the incompleteness for this particular sample as discussed above). Nonetheless, at a given M type the *JHK* colors are systematically bluer than those of nearby stars (FPAM), though not by as much as indicated by FW, since in Paper III we find that part of the difference noted by FW arose from differences in the classification schemes for bulge and local M giants.

To calculate *integrated* mean colors, indices, and magnitudes for all M stars (i.e., to predict how the entire ensemble of M stars would appear from a distance), weights were assigned to each of the three spectral subclasses in proportion to their relative numbers in the grism surveys. These mean colors for each latitude are given in Table 8. The integrated K-magnitudes are normalized to the area of one grism field by weighting the calculated integrated flux for all M giants found in the grism surveys by the inverse of the size of each field (the area surveyed at each latitude in units of one grism field is also given in Table 8). Entries for the −4° window are from Table 4 of FW with a minor arithmetical error corrected.

Figure 1 illustrates the results from Table 8. The *JHK* colors and H_2O indices are nearly constant for the four lower latitude fields, then become markedly bluer and weaker in the two high-latitude ones. The similarity in the variation of the H_2O index and $H-K$ color is consistent with the strong effect H_2O absorption has on this color. About three-quarters of the variation in $J-K$ is due to the $H-K$ change. In the remainder of this section we will attempt to interpret the color and index gradients in terms of a metallicity gradient in the bulge.

b) *Color-Magnitude Diagrams and the $J-K$ Colors*

The $J-K$ color of globular cluster giant branches increases monotonically with increasing [Fe/H] at constant luminosity (Frogel, Cohen, and Persson 1983, hereafter FCP83). Figure 2 presents reddening-corrected color-magnitude diagrams for the six bulge fields. While there are no striking differences between them, some trends may be noticed. Luminous red stars are present in the −4° and −6° fields but, as pointed out earlier, not at higher latitudes (they are absent from the −3° field probably because of the small number of stars observed and the extreme crowding on the grism discovery plate; FW found the brightest and reddest stars in the infrared in Baade's window to be among the faintest in the BMB survey). There appears to be increased scatter at the faint end of the *C-M* diagrams for the two highest latitude fields, probably due to field star contamination. There are very few stars brighter than $K \sim 6.5$ mag in any of the windows. It is possible that the brightest stars, particularly in the higher latitude windows, are foreground or disk stars (see § IV).

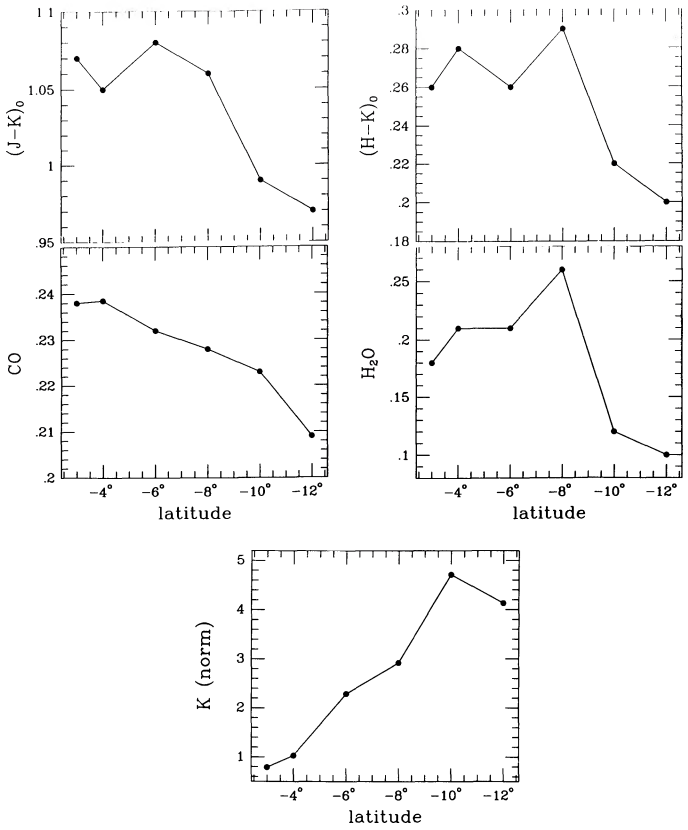

FIG. 1.—These five panels illustrate the variation with latitude of the *integrated* colors, indices, and normalized K-magnitudes for M giants in the six bulge fields, i.e., the values that would be observed if individual stars were not resolved. The uncertainties in these values are dominated by counting statistics and are no worse than ±0.02 for $J-K$, ±0.015 for $H-K$, ±0.01 for CO, and ±0.03 for H_2O. Data are from Table 8. The numbers of stars at each point are given in Table 7 or Table 11. The change in CO is consistent with that inferred from Table 9.

With the possible exception of the −12° field, the ridgelines of all of the *C-M* diagrams in Figure 2 lie close to that of 47 Tucanae and in no case lie redward of M67 or blueward of M3. Normally, e.g., for globular clusters, a sequence of decreasing metallicity should result in hotter and bluer giant branches. From the colors presented in Tables 7 and 8 we see that the mean integrated $J-K$ values for the bulge fields do get somewhat bluer with increasing latitude, as would be expected from the optically determined abundance gradient in the bulge (van den Bergh and Herbst 1974; Terndrup 1988). On the other hand, the range in metallicities that would be deduced from the color sequences in Figure 2 are considerably smaller than those found from optical spectra (Rich 1988). A similar effect seen in the Baade's window field was interpreted by FW (see also Frogel, Whitford, and Rich 1984) as the result of unidentified blanketing agents or peculiarities in the atmospheres of the bulge stars. Colors that are bluer than expected for the spectroscopically deduced metallicities are also seen in optical photometry of bulge stars (Terndrup 1988). This effect may be related to the result of FCP83 that the position of the giant branch of a metal-rich globular cluster in a (K, $J-K$) diagram is relatively insensitive to changes in [Fe/H]. We return to this discussion in § III*e*.

To examine these results in more detail, we computed $J-K$ distributions in bins 0.04 mag wide for bulge giants in the restricted magnitude range $-2.5 \geq M_{bol} \geq -4.5$. Biases intro-

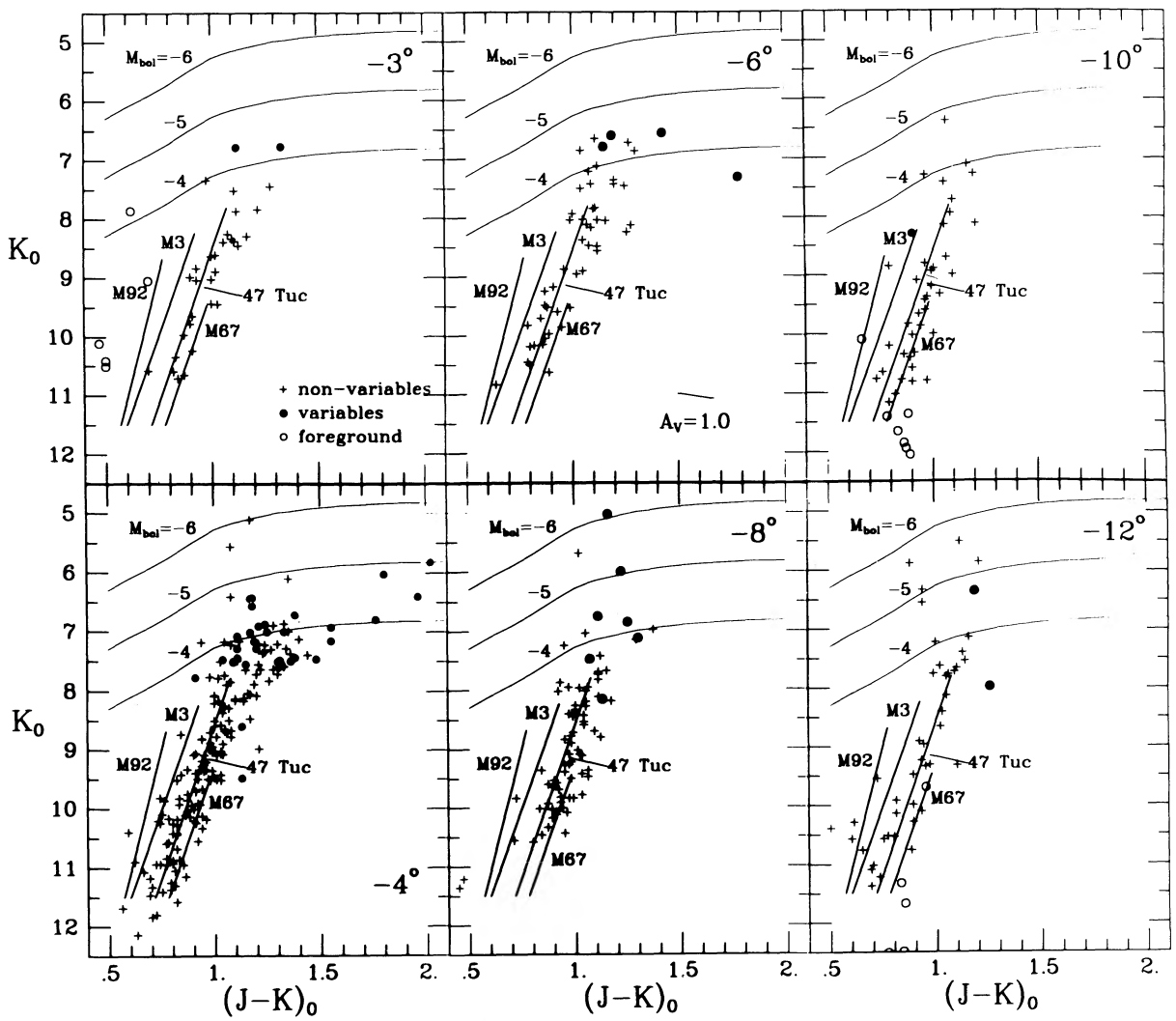

FIG. 2.—(K, $J-K$) color-magnitude diagrams for the six bulge fields. The fiducial cluster giant branches are from Cohen, Frogel, and Persson (1978), and Frogel, Persson, and Cohen (1981). Lines of constant bolometric magnitude are shown. Stars considered to be foreground objects are indicated. The effect of 1 mag of visual extinction is also indicated.

duced by our star selection process were removed by normalizing the number of stars in each of the three spectral groups for each field to take into account the number actually observed in a particular group relative to the number found in the essentially complete grism surveys. In other words, the normalized distributions should be equivalent to those that would be obtained if every M giant with $-2.5 \geq M_{bol} \geq -4.5$ found in the surveys had been observed. The distributions for the three lower and the three higher latitude fields were summed and are plotted in the upper and lower panels, respectively, of Figure 3.

The weighted mean colors of the distributions in the lower and higher latitude fields are $J-K = 1.09$ and 1.05, respectively. This difference is not caused by a change in the mean colors of the three spectral groups, which are independent of latitude (Tables 7 and 8); rather, it is the relative numbers of M stars of different types that are changing with latitude. The difference in the two means is only about half of the HWHM of the distributions and is due primarily to the relative scarcity of red giants with $J-K \geq 1.2$ in the higher latitude fields. As may be seen from Figure 3, such red giants are almost all of class M7–M9. These latest M stars are 2–3 times more numerous relative to the total M star population in the lower latitude fields than they are in the higher ones. Thus any metallicity gradient in the bulge has only a small effect on the integrated $J-K$ color of the M giants, essentially no effect on giants of a particular subclass, but a large effect on the presence or absence of the reddest, latest type stars. These new results are in qualitative agreement with Blanco's (1988) analysis of the dependence of numbers of late M giants on latitude, and they considerably strengthen the preliminary conclusion of Frogel, Blanco, and Whitford (1984), who found a steep latitude dependence for these stars based on data for only the $-4°$ and $-8°$ windows. Table 7 shows that the M7–M9 stars are the most luminous giants in the bulge and that their mean K-magnitude is independent of latitude. Therefore, *it is only the reddest, most luminous late M stars that have the steepest latitude dependence.*

Although the shift in integrated mean $J-K$ color with latitude is small, it may introduce a systematic bias in the completeness of the grism surveys at the higher latitude fields. This possibility arises because the color distributions are sufficiently

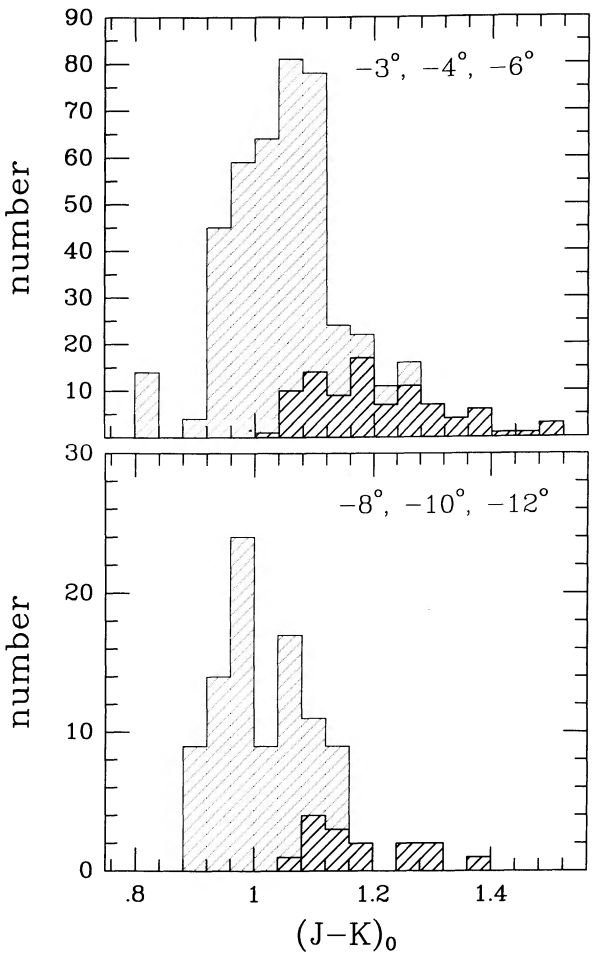

FIG. 3.—Normalized $J-K$ distribution of M2–M9 giants with $-4.5 \geq M_{bol} \geq -2.5$ for the three low-latitude bulge fields and the three high-latitude ones. The distributions for the M7–M9 stars are shown explicitly by the more boldly shaded areas of the panels.

wide that an increasingly significant fraction of the luminous giants, namely, those with warmer temperatures and weaker molecular bands, would not be detected in the grism surveys. In fact, visual inspection of the grism plates and direct photographs of the high-latitude fields shows a number of bright stars that, based on a quick CCD spectroscopic survey, are indeed early M and late K stars. Most of these are in the $-12°$ field. We have not yet been able to determine how many of these are foreground disk stars. In any case, their presence will not alter the main conclusions of this study.

c) *The CO Index*

The CO index, an indicator of the strength of the first-overtone absorption band of CO (band head at 2.29 μm), is positively correlated with metallicity in cool giants of similar temperature, such as those in globular clusters (FCP83) and in open clusters (Houdashelt *et al.* 1990). These giants cover a range in [Fe/H] from 0.0 to less than -2.0. The independently derived dependence of CO on [Fe/H] for open clusters at the high end of the metallicity distribution (Houdashelt *et al.* 1990) is nearly identical to that for globular clusters at the low end. One might expect that the CO indices of the bulge giants will also depend on [Fe/H]. Figure 4 shows that stars in all bulge fields have CO indices that are systematically greater than the mean relation for field giants at the same $J-K$, that the displacement from this mean relation increases with decreasing latitude, and that the dispersion of the CO index for stars within a field appears to be small. The reddening vector drawn on one of the panels indicates that systematic differences in the CO index from window to window cannot be attributed to reasonable uncertainties in the reddening.

To quantify the variations in the CO index seen in Figure 4, we selected stars with $0.85 \leq J-K \leq 0.95$ so as to exclude most variables and to minimize variations due to temperature, but still to be left with a reasonable number of giants for each window. The second column of Table 9 gives the mean CO index and its dispersion for the M giants in this color range for each bulge field. Similar values are obtained, although with more scatter and a systematic downward shift of 0.03 mag, if the $J-K$ interval chosen is moved blueward to 0.75–0.85.

The dispersion in the CO indices (Table 9) for a given field is only marginally greater than expected from measuring uncertainties alone. Rich (1988; see also Whitford and Rich 1983) finds a total spread of nearly 2 dex in [Fe/H] for K giants in Baade's window with an rms scatter of about ± 0.5. Equation (5) of FCP83 relates the measured CO index with [Fe/H] for globular cluster giants as follows:

$$\mathrm{CO} = 0.16 + 0.074[\mathrm{Fe/H}] .$$

A nearly identical relation is derived from observation of giants in old disk clusters with [Fe/H] between -0.6 and 0.0. From this equation we find that a ± 0.5 rms scatter in [Fe/H] corresponds to a dispersion in CO of ± 0.037, about twice that observed in the fields. Thus, either the distribution in [Fe/H] from optical spectroscopy may be overestimated, or there are other factors affecting the CO distribution within a given field (§ III*d* below), or equation (5) of FCP83 cannot be linearly extrapolated to higher metallicities.

It is worthwhile to emphasize the fact that the M giants are sampling *all of the bright giants* with the possible exception of the highest latitude fields. That this is true can be determined from examination of our visual charts for the field or, for example, the photometry of Arp (1965) and van den Bergh and Herbst (1974). Essentially all visually bright stars not selected out as M giants have $B-V$ too blue to be anything but early-type foreground stars. This result is important because, if there were a significant metal-poor component to the stellar population in the bulge, they would become K giants with M_{bol} as bright as -3.6 by analogy to globular cluster stars. If such a population were younger than globular clusters, the K giants would be even brighter. The fact that there are no such stars in the bulge fields means that all of the fainter K giants in Rich's (1988) sample must become M giants as they evolve up the giant branch and the asymptotic giant branch (AGB). Thus, as long as the earlier M giants are not excluded from the sample, the metallicity distribution of the whole sample of M giants must be typical of the bulge as a whole.

The mean CO strength increases by 0.04 mag between the highest and the lowest latitude field. Again using the above equation as a guide, we find that this corresponds to a change in [Fe/H] of 0.5. The FCP83 relation between CO and [Fe/H], as well as that of Houdashelt *et al.* (1990), is based on stars with $V-K$ near 3.0 or $J-K$ about 0.75. There are few stars in the bulge samples as blue as this. However, from the data in Frogel, Persson, and Cohen (1983) for globular cluster stars, we estimate that for the $J-K$ range being considered here,

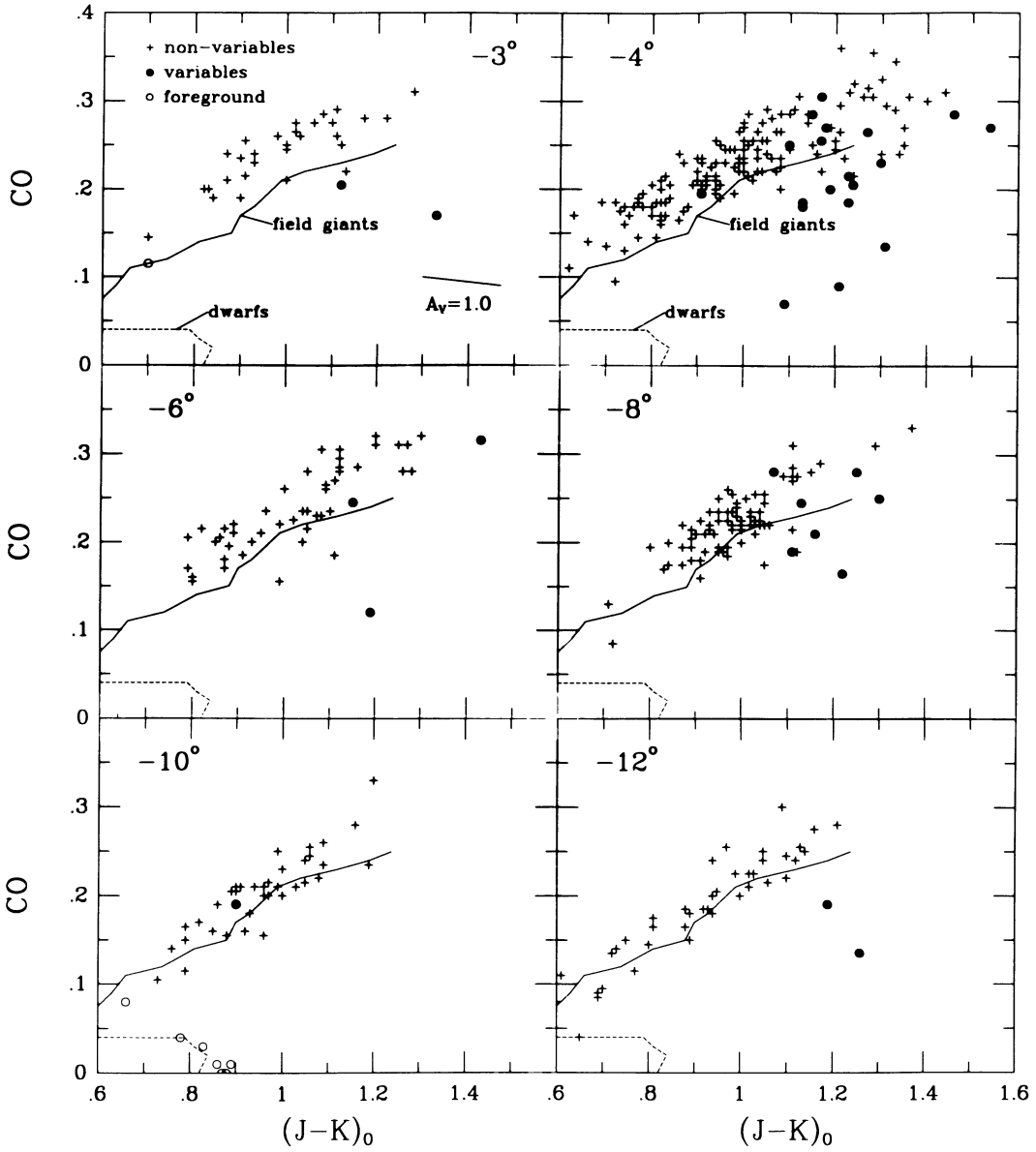

FIG. 4.—Dependence of CO on $(J-K)_0$ for M giants in the six bulge fields. Data are from Tables 2–6 and from FW. Both the −4° and −6° windows have a few stars redder than the limits of the plot. The effect of 1 mag of visual extinction is indicated on one of the panels.

TABLE 9

CO INDEX FOR GIANTS AND DISPERSION IN Δ-Δ PLOTS

FIELD	$\langle CO \rangle \pm \sigma$ $(0.85 \leq J-K \leq 0.95)$	DISPERSION IN Δ-Δ		
		$\Delta(H-K)$	Δ(CO)	σ(Δ(CO))
−3°	0.227 ± 0.019	0.027 ± 0.031	0.057 ± 0.020	±0.014
−4°	0.212 ± 0.021	0.044 ± 0.026	0.041 ± 0.021	±0.019
−6°	0.199 ± 0.015	0.007 ± 0.031	0.038 ± 0.028	±0.021
−8°	0.206 ± 0.022	0.022 ± 0.033	0.027 ± 0.024	±0.021
−10°	0.189 ± 0.020	0.012 ± 0.030	0.017 ± 0.017	±0.013
−12°	0.187 ± 0.021	−0.037 ± 0.031	0.012 ± 0.021	±0.012

0.85–0.95, the CO index will be 25%–30% more sensitive to metallicity changes than for the bluer stars used by FCP83. In this case the range in [Fe/H] between the $-3°$ and $-12°$ bulge fields based on the values in Table 9 will be reduced to 0.4 dex, consistent with the difference of 0.5 dex between the $-4°$ and $-10°$ fields that Terndrup (1988) finds from optical *C-M* diagrams. In addition, the decrease in $H-K$ with increasing latitude will cause the observed CO index to reflect only part of the true change in the CO absorption because of the single-sideband nature of the index (FW). Since $H-K$ of globular cluster giant branches is almost independent of metallicity, the actual change in [Fe/H] will be somewhat greater than 0.4 dex.

Can we estimate an absolute value of [Fe/H] from the observed indices of the bulge giants? Allowing for the greater sensitivity of the CO index to metallicity changes for the color range considered here relative to that in FCP83, we find that for the two innermost fields the CO index implies an [Fe/H] of about $+0.1$, while for the two outermost fields it is about -0.3 or -0.4. Alternatively, we can use the CO indices of the bulge stars with colors similar to those used to derive the relation between CO and [Fe/H] in FCP83.[4] Although only a few stars this blue were observed in the bulge, implying a relatively larger uncertainty in quantities derived from data for these stars, we find that their CO indices imply a range in [Fe/H] of from 0.0 to -0.6 in going from the inner to the outermost fields. These estimates are consistent with the metallicity gradient found by Terndrup (1988) and the absolute values for the mean metallicity derived by Rich (1988) and Terndrup. While the slight reduction in [Fe/H] values from the somewhat redder sample may not be statistically significant, it is qualitatively consistent with our cautionary note expressed just above. Finally, we caution that the metallicities estimated for the bulge stars ignore the fact that their *JHK* colors appear to be affected by blanketing agents not present in solar neighborhood or globular cluster stars. This issue will be addressed in §§ III*d* and III*e* below.

d) The $(J-H, H-K)$ Relation

Stars from different population groups that differ from one another in terms of their mean metallicity have differing mean $(J-H, H-K)$ relations. For example, the high-metallicity M giants in Baade's window lie on the side of the mean relation for solar neighborhood field giants opposite to that for globular cluster stars (FW). M giants in the Large Magellanic Cloud, which most likely have a lower metallicity than solar neighborhood stars, also lie on the globular cluster side of the field giant line (Cohen *et al.* 1981). Figure 5 shows the $(J-H, H-K)$ colors for bulge M giants. There is a steady progression from one side of the local field line to the other as we go from low to high latitude. Nearly all of the stars from the $-3°$ and $-4°$ fields lie on the side opposite to that on which the globular cluster giants are found, whereas all but a few of the giants from the $-12°$ field scatter about a line representative of the location of most globular cluster giants. The scatter within a given field is generally small.

We attribute the changing location of the stars in the six panels of Figure 5 to a metallicity gradient in the bulge. The overlap of the $-12°$ stars with the globular cluster distribution is consistent with the behavior of the CO index with latitude discussed in the previous section. This smoothly varying behavior of bulge to globular cluster giants in the $(J-H, H-K)$-plane raises the possibility that the source of the continuous or line opacity that most influences these colors is the same for the two populations and that it is a result of metallicity differences alone.

Is there a correlation between the displacements of bulge stars from the CO and $H-K$ mean field giant lines in Figures 4 and 5? For each of the six bulge fields we formed a subset of the data from Tables 2–6 and from FW. First, stars with H_2O indices strong enough to affect either CO or $H-K$ were eliminated; i.e., those with any one of $J-K > 1.1$, $H-K > 0.35$, $J-H < 0.65$, or $H_2O > 0.20$. Then at constant $J-K$ and $J-H$ the displacement of each star from the mean lines in CO and $H-K$, defined as $\Delta(\mathrm{CO})$ and $\Delta(H-K)$, respectively, was determined. The six panels of Figure 6 show the resulting Δ-Δ plots for the fields. The mean of and dispersion in the values of $\Delta(\mathrm{CO})$ and $\Delta(H-K)$ for the sample of stars in each of the fields—excluding the few obvious outliers in Figure 6—are given in the third and fourth columns of Table 9.

A least-squares regression analysis demonstrates that the dependence of $\Delta(\mathrm{CO})$ on $\Delta(H-K)$ for individual stars is significant at least at the 98%–99% level for each of the windows. The slopes of the individual solutions vary from 0.22 to 0.39, with a mean value of 0.28 ± 0.08. This dispersion about the mean is consistent with the uncertainties in the individual slope determinations, indicating that there is no measurably significant variation in the slope from window to window. The last column of Table 9 gives the dispersion in $\Delta(\mathrm{CO})$ about the least-squares line in the Δ-Δ plots for each field; this is denoted as $\sigma(\Delta(\mathrm{CO}))$. These $\sigma(\Delta(\mathrm{CO}))$ values are slightly smaller than those that would be obtained if the dependence of $\Delta(\mathrm{CO})$ on $\Delta(H-K)$ were not removed, i.e., the dispersions in the individual $\Delta(\mathrm{CO})$ values given in the penultimate column of the table. We interpret the correlation between $\Delta(\mathrm{CO})$ and $\Delta(H-K)$ as arising from the effects of star-to-star metallicity differences within a window. In each window the dispersion in either quantity, however, is comparable to the observational uncertainties alone; thus the $\Delta(\mathrm{CO})$ and $\Delta(H-K)$ values for any one star cannot be used to infer that star's metallicity.[5]

Smith (1988) has shown that for metal-rich field stars a similarly measured $\Delta(H-K)$ correlates with the strength of the 4215 Å CN band, although the size of the effect is small. His

[4] That all fields have a mean CO strength greater at a given $J-K$ color than the field giant line does not necessarily imply an [Fe/H] greater than solar for the fields. Equation (5) of FCP83 yields a value of CO = 0.16 for globular cluster stars with $V-K = 3.0$ and [Fe/H] = 0.0. On the other hand, the mean relation for field giants (Frogel *et al.* 1978) gives a value for CO of 0.12–0.13 at this color. Figure 7 of Frogel, Persson, and Cohen (1983) illustrates this difference for NGC 5927. One possible origin of the difference would be if the giants that went into defining the mean field star relation were of lower luminosity than the giants in metal-rich globular clusters, since CO increases with increasing luminosity at constant metallicity. This does not seem likely, however, as one would expect field giants to be more luminous than their globular cluster counterparts of similar temperature and metallicity, since the former stars must be younger than the latter. Another possibility would be systematic differences in the microturbulent velocity in the atmospheres of solar neighborhood and globular cluster stars. Since the CO bands contain many saturated lines, a higher microturbulent velocity will increase the observed strengths of the bands (Frogel 1971).

[5] Can the metallicity component (in contrast to the observational uncertainty component) of the Δs be seen in the *C-M* diagrams? We considered small subsets of stars with the (algebraically) smallest values of Δ from each of the bulge fields in Fig. 6. For some of the windows a weak tendency could be seen for these stars to lie preferentially on the blue side of the *C-M* distribution for all of the stars in a given window in Fig. 2. The uncertainties are large enough, and the effect appears to be small enough, that this result cannot be quantified.

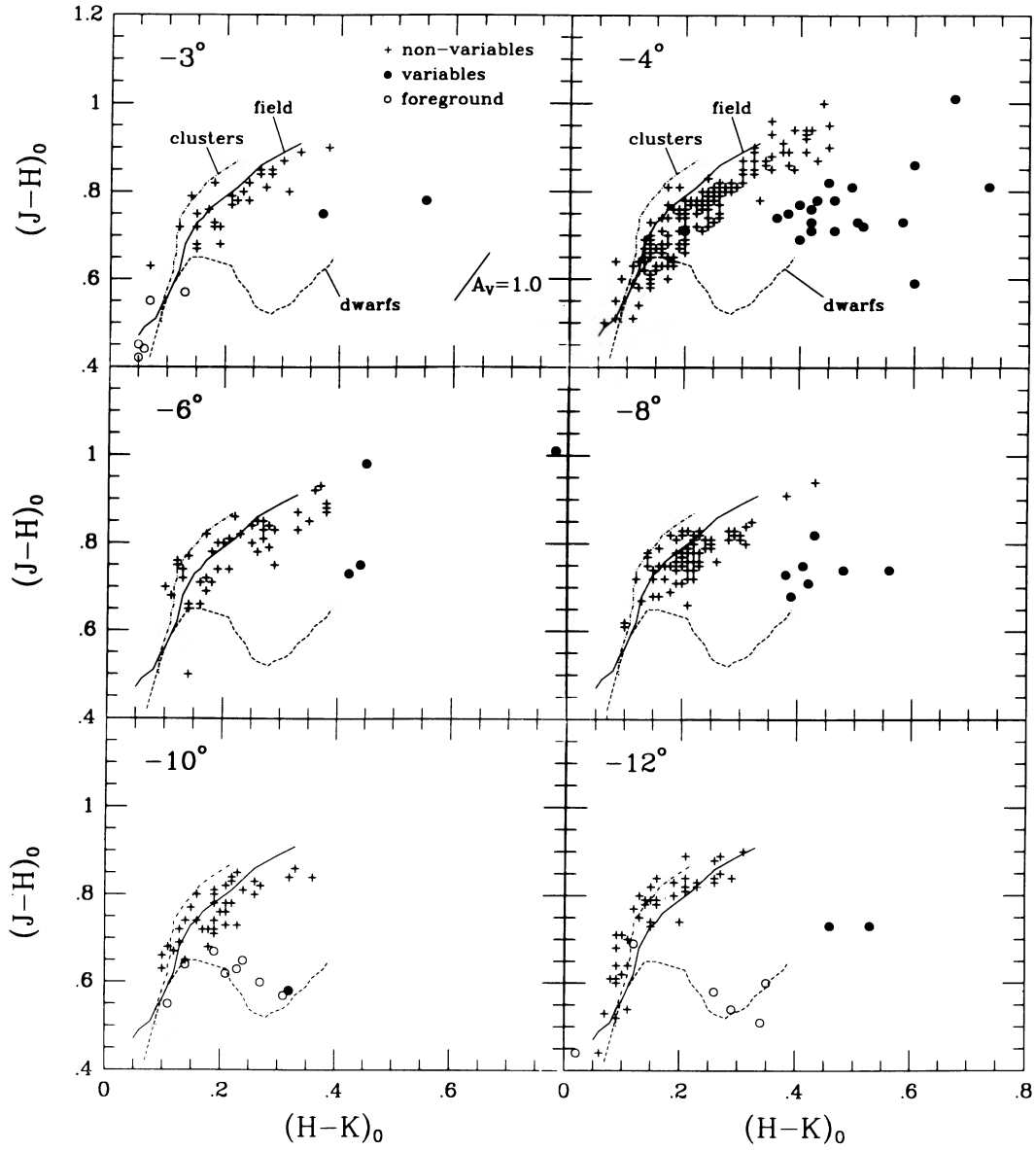

FIG. 5.—The six panels of this figure illustrate the relation between $(J-H)_0$ and $(H-K)_0$ for M giants in the six bulge fields. Data are from Tables 2–6 and from FW. Both the $-4°$ and $-6°$ windows have a few stars redder than the limits of the plot. Mean relations for field giants and dwarfs in this and succeeding figures are from FPAM and Aaronson, Frogel, and Persson (1978). The dot-dash line is the mean relation for the globular clusters M3, M13, M71, M92, and 47 Tuc. The effect of 1 mag of visual extinction is indicated by the vector in one of the panels.

analysis, therefore, supports the interpretation that the relative locations of stars in the $(J-H, H-K)$-plane is metallicity-related. Smith's equation (2) indicates a range in [Fe/H] [from the spread in the $\Delta(H-K)$ values of Table 9] from the lowest to the highest latitude field of about 0.5 dex, once more consistent with that derived from the CO indices.

Finally, we note from Table 9 that the full widths of the distributions of CO and $H-K$ within any of the windows is of a size comparable to those of the differences in their mean values between the highest and lowest latitude windows. However, the dispersions within each window, given in Table 9, are only slightly larger than the measuring uncertainties (about 0.015–0.02). Thus it appears that the spread in CO and $H-K$ *within* a window could be less than that observed *between* the six windows. Saturation effects in the CO absorption bands could limit the maximum strength observed and, at the same time, make the spread within a window appear artificially small. Now from optical photometry Terndrup (1988) finds a difference in [Fe/H] of -0.5 dex between the $-4°$ and $-10°$ fields. The difference between fields at $-3°$ and $-12°$ should be comparable or somewhat greater. Rich (1988) finds from spectra of K giants in Baade's window an rms scatter in [Fe/H] of about 0.5 dex. The indication from their work, then, is that the *intra*window dispersion in [Fe/H] is comparable to or greater than the *inter*window dispersion.

Our analysis of the data in this paper shows that the variation in the mean values of the infrared parameters as functions of latitude are indicative of metallicities comparable in absolute value and gradient to those deduced from optical studies. But as noted in FW, variations in infrared colors and indices *within* a window are hard to reconcile with the optically determined intrawindow spreads in [Fe/H] (Rich 1988; Terndrup

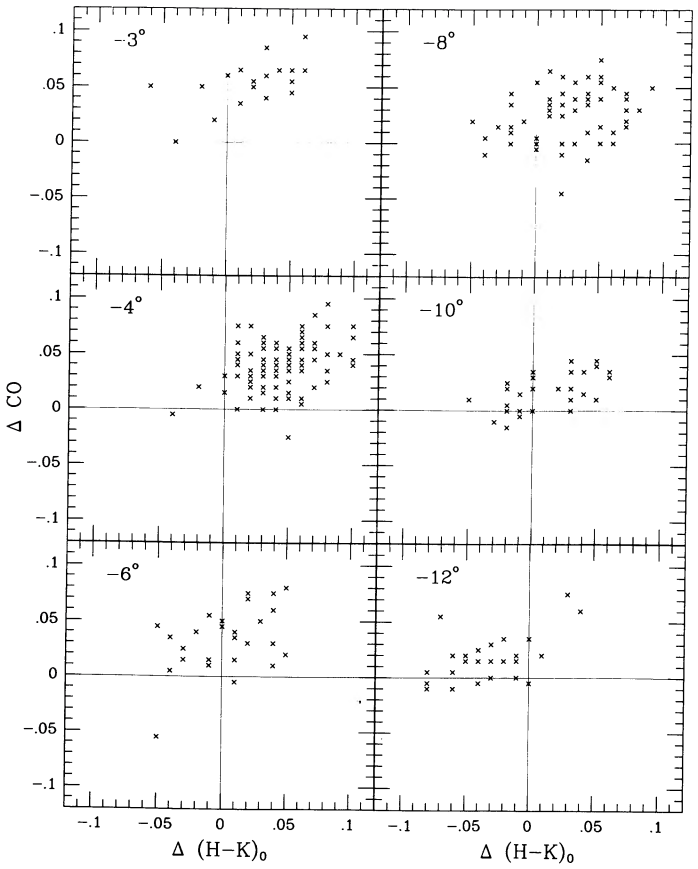

FIG. 6.—Displacement from the mean field giant lines of the CO index and $H-K$ color, at constant $J-K$ and $J-H$, respectively, of bulge stars with $J-K \leq 1.1$ and $H-K \leq 0.35$ is illustrated for each bulge field.

1988). A possible reconciliation is that the bulge M giants may have a somewhat narrower and more metal-rich [Fe/H] distribution than the K giants, since the evolutionary tracks of the most metal-poor stars will not be cool enough to enter the M giant domain. On the other hand, Rich's spectroscopic estimates of [Fe/H] for the most metal-rich K stars have to rely on extrapolation so that the spread in [Fe/H] may be overestimated. The first possibility is unlikely, since, as argued in § III*c*, the M giants should not be biased as to metallicity because there is no evidence of any luminous K giants in the fields; such stars would be the expected progeny of any significant metal poor population. A resolution of this difference between conclusions drawn from the optical and infrared data will require a better understanding of the continuous and molecular opacity in the bulge stars.

e) Narrow-Band Colors

For 33 of the M giants in the −3°, −6°, and −12° fields a 102 − C220 (see FW, § IV) color was determined. These data are given in Tables 2, 3, and 6, respectively. The 102 measurement refers to a filter centered at 1.015 μm with a 0.05 μm wide bandpass. The C220 measurement is made with a continuously variable filter (CVF) positioned so as to pass light at 2.20 μm with a FWHM bandpass of 0.03 μm (see FW for more details about the choice of these wavelengths). This narrow-band 102 − C220 color is designed to measure the (presumably) unblanketed continuum and thus to help separate the effects of varying metallicity and temperature on the broad band infrared colors and indices of the stars.

The two panels of Figure 7 show the dependence of $J-H$ and $H-K$ on 102 − C220 for bulge giants; data for Baade's window are taken from Table 6 of FW. From this figure it is apparent that at constant 102 − C220 the effect of metallicity differences between the fields is considerably greater in $J-H$ than it is in $H-K$. Furthermore, the location of the stars from the various fields indicates that the latitude dependence of these effects is of opposite sign for the two colors. To quantify the shifts in the colors, we took the 38 stars in Figure 7 with 102 − C220 ≤ 2.1, determined their least-squares dependence on 102 − C220, and, for each field, calculated the mean displacement in $J-H$ and $H-K$ of the stars from the least-squares line. Table 10 gives these values together with their dispersions. A trend is obvious for $J-H$ but is weak for $H-K$, although it is probably present. The associated dispersions are consistent with values expected from measuring uncertainties alone.[6] This behavior is similar to that seen for the intrawin-

[6] Observational uncertainties will be greater in $J-H$ than in $H-K$ because of greater sensitivity to reddening and because the J filter is much more affected by atmospheric extinction than the other two filters. Nevertheless, the small dispersions in observations made over a period of several years testifies to their high degree of internal accuracy; if, in fact, all of the $\Delta(H-K)$ values are considered together, their dispersion is only 0.016 mag.

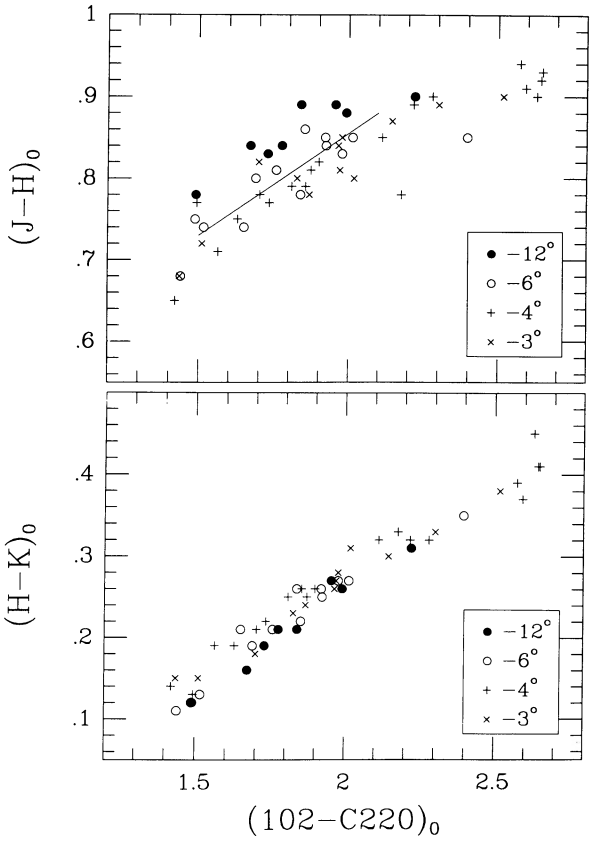

FIG. 7.—The two panels of this figure show the dependence of the $J-H$ and $H-K$ broad-band colors on the narrow-band color 102 − C220 chosen to be relatively free of blanketing effects. Data for the −4° window are from FW. The line represents the least-squares fit to the data for stars with 102 − C220 between 1.5 and 2.1.

TABLE 10

DISPLACEMENT FROM MEAN LINE FOR 102−C220

Field	$\langle\Delta(J-H)\rangle$	σ	$\langle\Delta(H-K)\rangle$	σ
3°.....	−0.019	0.028	0.004	0.014
4°.....	−0.017	0.024	0.014	0.011
6°.....	0.00	0.024	−0.003	0.015
12°.....	0.048	0.015	−0.015	0.010

dow dispersions in CO and $H-K$ (§ III*d*). Thus, once again the intrawindow metallicity dispersion observed in the optical by Terndrup (1988) and Rich (1988) is not reflected in the infrared data.

FW compared the 102−C220 colors of Baade's window M giants to ones in the solar neighborhood and found that metallicity differences between the two samples had a significant effect on the H and K filters but not at J. Our results are consistent with FW's since it may be deduced from Figure 7 that these effects are greatest in the H filter. The displacement in $J-H$ at constant 102−C220 (assumed to be relatively unaffected by metallicity differences between stars of the same effective temperature) with increasing latitude is in the same direction as the shift observed in going from Baade's window to field giants. We conclude that, *as a result of blanketing differences in the JHK filters, J−K will become bluer with decreasing latitude, i.e., with increasing metallicity.* Thus we have a clear demonstration of the effects of metallicity on infrared color-magnitude diagrams of bulge M giants, namely, metal-rich stars from one field will be shifted to the blue with respect to stars from another field even though the latter field has a lower mean metallicity than the former.

Figure 8, a plot of the individual $\Delta(J-H)$ values determined from Figure 7 against the stellar H_2O indices, examines the role of H_2O as a blanketing agent. The temperature dependence of H_2O has been removed by the manner in which $\Delta(J-H)$ is defined; only the metallicity dependence should be left. We know that H_2O has a strong effect on the infrared

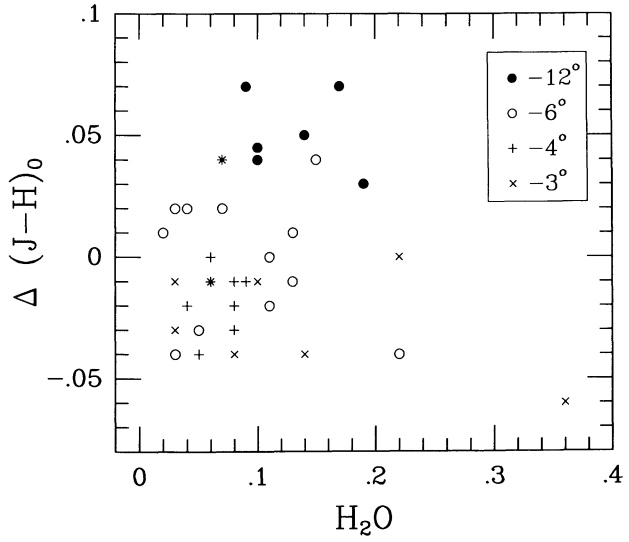

FIG. 8.—$\Delta(J-H)_0$ is the vertical displacement, measured positive upward, of the stars in Fig. 7 from the least-squares line in that figure. The H_2O indices are from the data in this paper or FW.

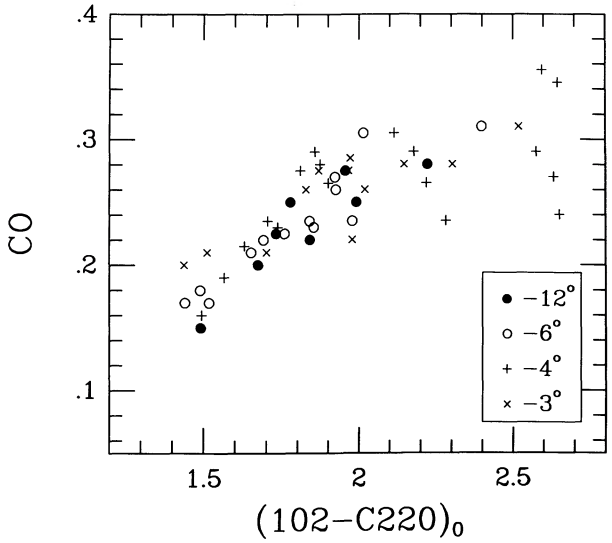

FIG. 9.—CO index plotted against the narrow-band 102−C220 color

colors of LPVs (Frogel and Elias 1988). FW suggested that this molecule is also an important contributor to the blanketing in the *JHK* filters for nonvariable bulge giants. Figure 8 shows, however, that for relatively low values of the H_2O index some other agent must be responsible for the differential absorption observed at different latitudes in the bulge, since at a given value of the index there is a spread in $\Delta(J-H)$ of 0.07 or greater with *no* clear trend visible. It is possible that part of the strong trend noticed by FW from their Figure 15*b* (note that FW measures displacement positive *downward* from a fiducial line, whereas here an *upward* displacement is positive) is due to their extrapolation of the mean line for field giants.

Finally, Figure 9 shows the dependence of CO on 102−C220. Given our previous discussion on the metallicity dependence of CO as a function of latitude, it is surprising that so little spread is seen in this figure. However, FW pointed out that there are blanketing effects even in the supposedly "clean" 102 filter. If we assume that these effects are strongest in the lowest latitude windows, then to correct for them the low-latitude stars must be shifted to the blue in Figure 9 with respect to the high-latitude stars. The result will be a greater difference in the CO index between stars from different latitudes than would be deduced from Figure 9.

The discussion in this section would seem to imply that the decrease in mean CO index with increasing latitude measured at constant $J-K$ (Table 9) is overestimated. While this implication is true, the effect will be offset somewhat by the fact that the "true" CO index (FW) is given by CO + $0.29(H-K)$; this correction will be greatest for the low-latitude stars. The net result is that the range in the values for $\langle$CO$\rangle$ given in Table 9 should probably be reduced by 20%–30%. However, given the uncertain nature of the state of our knowledge about blanketing and opacity effects in these stars, further refinements in the evaluation of these window-to-window differences in index and color values are unwarranted. Nevertheless, the trends are clearly established; a rigorous interpretation of them must await a more physical understanding and analysis of the opacity sources in these stars.

TABLE 11

LUMINOSITY FUNCTION FOR M GIANTS IN BULGE FIELDS

	log N					
M_{bol}	−3°	−4°	−6°	−8°	−10°	−12°
−6.20	...	...	...	0.00	...	...
−5.80	...	...	...	...	...	0.78
−5.40	...	...	...	0.01	...	0.78
−5.00	...	0.00	...	0.00	0.20	0.08
−4.60	...	0.30	0.78	...	...	0.00
−4.20	0.82	1.47	1.06	0.80	0.61	0.34
−3.80	0.00	1.71	1.32	0.70	0.00	0.00
−3.40	1.12	1.70	1.47	1.09	0.76	0.68
−3.00	1.01	1.89	1.37	1.22	0.66	0.34
−2.60	1.50	2.02	1.31	1.17	1.03	1.08
−2.20	0.96	2.36	1.77	1.23	0.94	1.38
−1.80	1.24	2.40	1.62	1.49	1.18	1.33
−1.40	1.25	2.55	1.88	1.49	1.14	1.40
−1.00	1.09	2.41	0.70	0.87	1.08	1.03
−0.60	...	2.40	...	...	0.79	0.08
N(obs)	31	143	51	81	38	44
N	119	1659	294	144	85	127
Dispersion (FWHM)	0.19	0.23	0.40	0.54	0.63	0.80

IV. LUMINOSITY FUNCTIONS

The bolometric luminosity function for each bulge field is given in Table 11; that for Baade's window is from FW. The first column of Table 11 is the central magnitude for each 0.4 mag bin. The luminosity of every observed star in a window was assigned a weight equal to the number of giants with the same spectral class found in the grism survey of that window, divided by the number of that class with infrared data. The last three lines in Table 11 summarize, respectively, the number of M giants in each window with infrared observations, the adjusted total number of M giants found by the grism surveys, and the front-to-back dispersion in the windows (FWHM in magnitudes) expected for a density law that matches the observed star counts at each latitude (cf. Terndrup 1988). Incompleteness should not be a significant factor except for the earliest M giants (BMB; Blanco 1987); in all cases, though, there will be no significant error in the luminosity functions for $M_{bol} \leq -1.4$ in the lower latitude windows (FW). On the other hand, as discussed earlier, it is possible that in the highest latitude windows some bright late K or early M giants may have been missed. Finally, since all known LPVs in the windows were found during the course of the grism surveys, they are automatically included in Table 11 and required no special attention. This differs somewhat from the procedure for Baade's window (FW).

The luminosity function (LF) for Baade's window is used to intercompare the LFs for the other fields since it is the best determined. Because of the increasing dispersion in magnitudes along a line of sight through the bulge with increasing latitude, the Baade's window function was smeared out by a Gaussian that took into account the differences in dispersion given in Table 11. The main effect of this smearing is to smooth out the LFs somewhat and deemphasize the peak near the faint completeness limit. Figure 10 compares the appropriately smeared-out Baade's window LF to those for the other fields. The difference in path length through the bulge at −3° and −4° is not significant, so the Baade's window LF was plotted directly on the −3° data. The total numbers of stars in each window have been scaled to match the number in Baade's window in

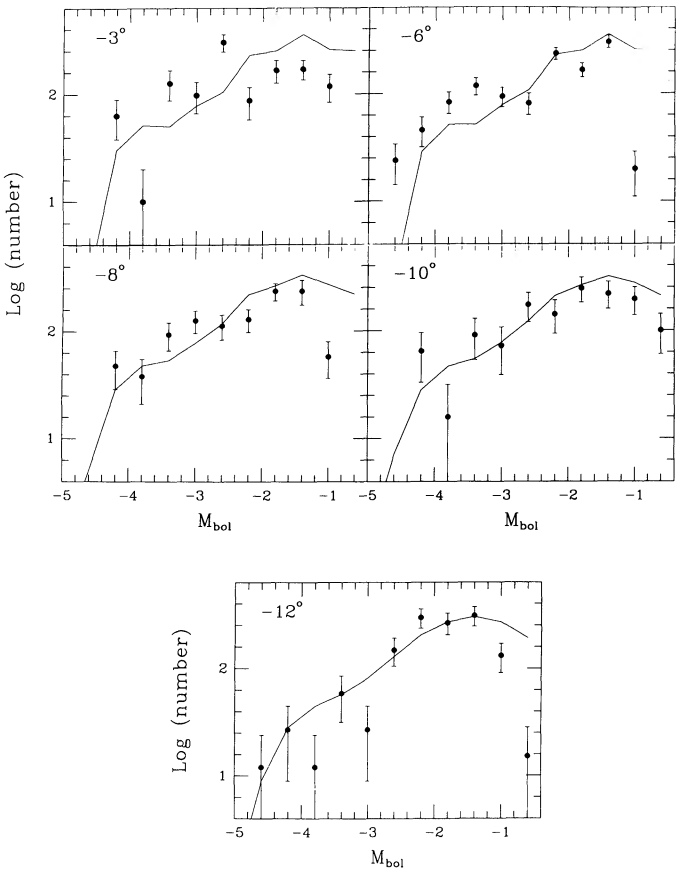

FIG. 10.—These five panels compare the luminosity function for each field with the Baade's window function. The latter has been smeared out to correspond to the path length through the bulge at the relevant latitude.

the range $-4.6 \leq M_{bol} \leq -1.4$. The error bars on the points reflect the appropriately scaled counting statistics.

Figure 10 shows that there are no significant differences in the luminosity function of bright bulge giants as a function of latitude. The apparent scarcity of stars fainter than M_{bol} of -1.8 in the $-3°$ window is an effect of the extreme crowding in this field and the resulting incompleteness for the fainter stars. The LFs for the $-6°$ and $-8°$ fields seem to have a small excess of stars near $M_{bol} \approx -3.4$. The LF for $-12°$ is perhaps flatter than for Baade's window, with a larger contribution from bright stars, though the errors are large (the bins for the $-12°$ field brighter than $M_{bol} = -4.6$ were not plotted in Fig. 10 but are given in Table 11). Since all of the LFs are similar, we show in Figure 11 the combined luminosity function for all windows, each weighted by the number of stars in that window with infrared photometry, and for all but the $-12°$ one. The path-length effect has not been included. The difference between the two LFs in Figure 11 is entirely due to the few bright stars in the $-12°$ field.

The similarity in LFs at different latitudes appears to conflict with the relatively rapid decline in numbers of the reddest and latest type M giants (Blanco 1988), which from Table 7 are seen to be the brightest stars in each window. What is happening is that the brightest stars are getting bluer with increasing latitude; they are not getting any fainter. This effect may be appreciated by inspection of the *C-M* diagrams in Figure 2. As we will show in Paper III, the spectra of these brightest stars in the higher latitude windows lead us to conclude that they are foreground stars. It appears that with increasing latitude the number of luminous bulge stars is decreasing at about the same rate as the number of foreground stars is increasing. In fact, it is possible that all stars with $M_{bol} \leq -4.2$ are foreground stars. The potential use of such a sharp cutoff as a distance indicator has been pointed out by FW. In any case, the LF in Figure 11 without the $-12°$ contribution is our best present estimate for the LF for the bulge.

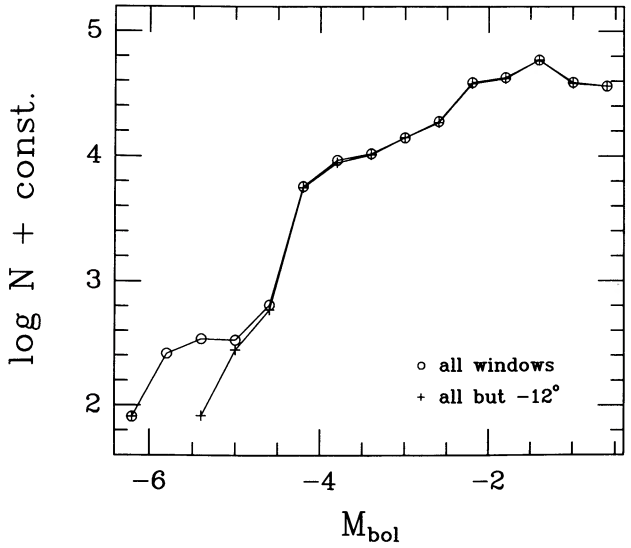

FIG. 11.—Combined bolometric luminosity function for all fields together and for all but the $-12°$ one. The contribution of each field to the luminosity function has been weighted by the number of stars in the field with infrared data. No account has been taken of the smearing effect due to the increasing path length through the bulge at higher latitudes.

V. LONG-PERIOD VARIABLES IN THE BULGE

a) Luminosity and Color

Long-period variables (LPVs) are easily distinguished on the basis of their infrared colors and indices from other types of variables and from nonvariables. This is true for globular cluster LPVs (Frogel and Elias 1988; Frogel 1983), for LPVs in Baade's window (FW), and for field LPVs (Feast *et al.* 1982). Within the boundaries of Blanco's (1987) $-8°$ grism field there are six variables (Plaut 1971), each of which could be identified with one of Blanco's M giants that we observed. These six stars stand apart from other stars in the $-8°$ field (see e.g., Fig. 5).

Three strong distinguishing characteristics of the optically identified LPVs in the $-4°$ and $-8°$ fields have been used as guides in identifying LPVs in the other windows and a new LPV in the $-8°$ field. These are a significant displacement from the location of other stars in the $(J-H, H-K)$-plane, strong H_2O indices (nearly all of the LPVs have $H_2O \geq 0.4$) and red $K-L$ color for their $J-K$ color. These characteristics are illustrated in the panels of Figure 12. Because of their red continuous energy distribution, the CO indices of the LPVs are often weaker than those of their non–LPV counterparts with similar broad-band colors. For each of the windows other than the $-4°$ and $-8°$ ones, one or more stars stood clearly apart from the rest in at least two of the three key characteristics. The stars so selected have a "V" attached to their spectral type in Tables 2–6 and are distinguished in various figures in this paper.

Table 12 lists the number of M giants in each window identified as LPVs. The entry for the $-10°$ field refers to V1889 Sgr located just outside of the grism survey field; no other variables were found in this field. The third column of Table 12 adjusts the numbers in the previous column to allow for the sampling statistics of the three spectral groups and normalizes to the area of one grism field. The last column of the table gives the flux-weighted mean bolometric magnitudes of the LPVs. For Baade's window this number differs somewhat from that in FW, since the sample considered has been slightly modified. Figure 13 illustrates the M_{bol} distribution for all known globular cluster LPVs (Frogel and Elias 1988 and references therein) and for the bulge LPVs; the two distributions have been normalized to the total number of LPVs in each.

The flux weighted $\langle M_{bol} \rangle$ for all bulge LPVs, weighted by the numbers in the third column of Table 12, is -4.2. In spite of some key differences between stars in the bulge and in globular clusters, e.g., the metallicity and the luminosity of the brightest nonvariable giants, *$\langle M_{bol} \rangle$ for bulge LPVs, -4.2, is statistically indistinguishable from $\langle M_{bol} \rangle = -4.1$ for all globular cluster LPVs.* Use of the somewhat greater Galactic center distance modulus that is indicated from radio observations would make the value for the bulge LPVs brighter by only a couple of tenths of a magnitude. This result implies that LPV luminosities cannot be used as an argument for a low age for bulge stars. Differences in metallicity between globular cluster and bulge stars result in the latter being somewhat more massive than the former for equal age and hence give the latter the ability to achieve a higher luminosity on the AGB (Frogel and Whitford 1982).

Some periods that have been estimated for bulge LPVs, including *IRAS* sources (Wood and Bessell 1983; Harmon and Gilmore 1987) are long enough to imply initial masses as great as 2.7 $M_\odot$, or an age, for solar metallicity, of ~ 0.5 Gyr. It is

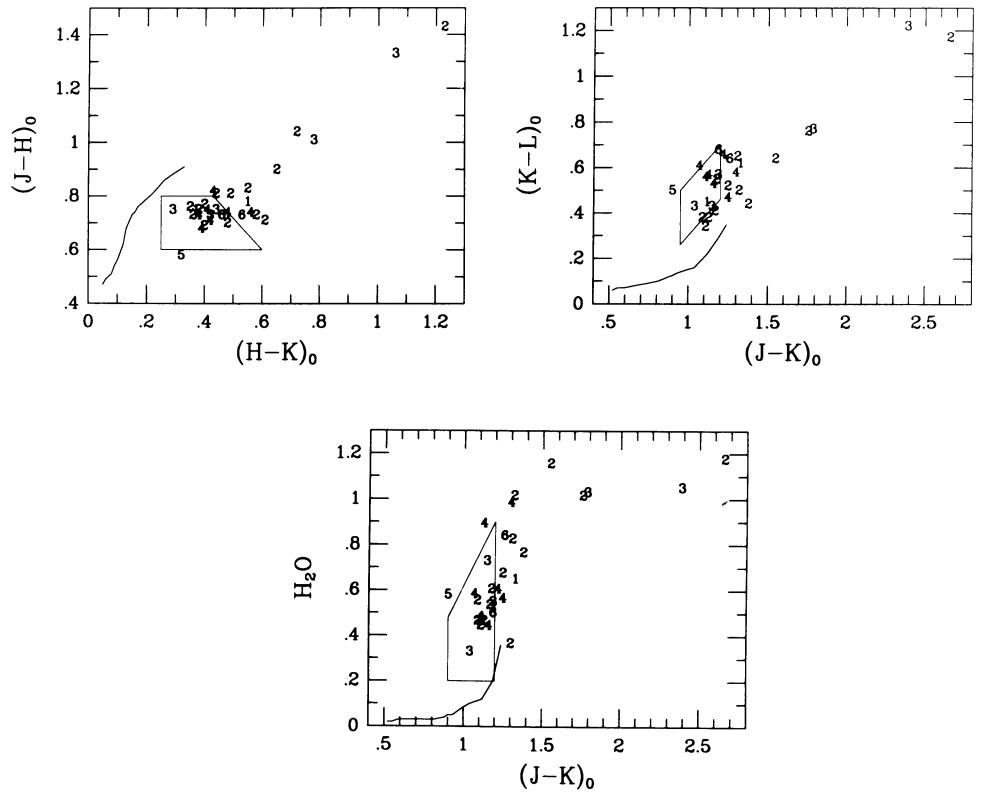

FIG. 12.—*JHKL* colors and H_2O indices for LPVs in the six bulge fields. The numbers identify which field a star is from: 1 is the lowest latitude, 6 the highest. Fiducial sequences for local giants together with the regions occupied by globular cluster LPVs are shown for reference.

easy to show that such a low age for AGB stars would imply a significant population of blue turnoff stars in the bulge. Such stars are just not present (van den Bergh and Herbst 1974; Rich 1985; Whitford 1986; Terndrup 1988). has set a lower limit of 5–8 Gyr for the age of bulge turnoff stars. If there was a significant population of intermediate-age stars in the bulge, it would produce a detectable population of luminous AGB stars. As we have already argued (Frogel and Whitford 1982; FW), the maximum bolometric luminosities observed for the bulge giants are consistent with the presence of a very metal-rich population. It is possible that these especially long-period LPVs are members of a disk population, since as many as 10%–20% of the late-type giants seen in the direction of the inner bulge are estimated to be disk stars (Blanco and Terndrup 1989) at various distances from us. Also within the central 1° of the bulge there appears to be a population of giants, including OH/IR stars, more luminous than any we have found (Lebofsky and Rieke 1987; Winnberg *et al.* 1985) as well. Alternatively, the high metallicity of the bulge giants may render the correspondence between period and mass moot. It

TABLE 12

LPVs IN THE BULGE FIELDS

Field	Number of Observations	Normalized Number of Observations	$\langle M_{bol} \rangle$
−3°	2	22	−4.28
−4°	14	16	−3.82
−6°	5	5	−4.19
−8°	7	9	−4.75
−10°	(1)	0	−3.36
−12°	2	0.6	−4.26
All	...	...	−4.2
Globular clusters	...	...	−4.1

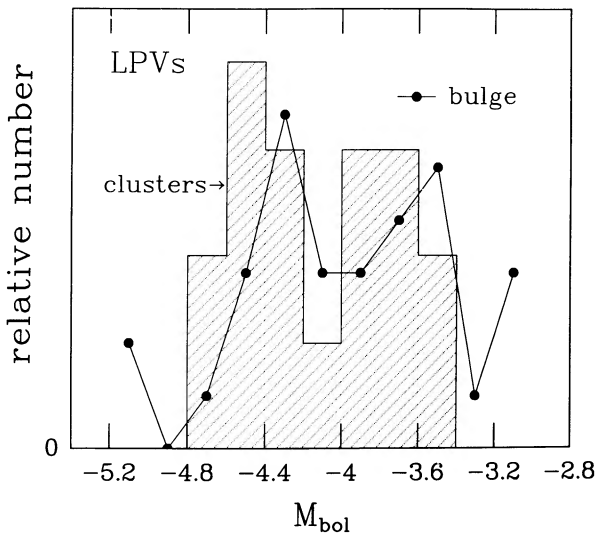

FIG. 13.—Normalized distributions of M_{bol} for bulge and globular cluster LPVs. The mean values of the two distributions are statistically indistinguishable.

would be useful to determine accurate periods for the bulge *IRAS* sources that Harmon and Gilmore (1987) have identified as LPVs, since their sample contains the stars with the longest periods.

b) *Properties as a Function of Latitude*

Figure 12 illustrates the only significant difference between bulge LPVs from the different fields: the maximum value of their redness and the strength of their H_2O indices. Those with the reddest colors and strongest H_2O indices come from the lowest latitude windows. Indeed, while the majority of LPVs lie in a relatively well-defined clump in Figure 12, the five reddest ones define tight sequences in the $(J-H, H-K)$ and the $(J-K, K-L)$-planes; these extend to colors far redder than observed for the latest non–LPV giants. Figure 12 also shows that the colors and indices of the globular cluster LPVs overlap those of the clump of bulge LPVs but that the latter have bluer colors and weaker H_2O indices.

As interpreted in FW, the red sequence of bulge LPVs in Figure 12 arises from the increasing contribution to the energy distribution from circumstellar dust with a characteristic temperature ~ 1000 K. That only lower latitude stars are found along this sequence points to a metallicity effect. Higher metallicity could lead to a larger dust-to-gas ratio in these stars for equal mass-loss rates; it could also enhance mass loss through, for example, radiation pressure on grains with a resulting greater amount of momentum transfer to the gas. Since Frogel and Elias (1988) found that LPVs in globular clusters have a relatively high mass-loss rate in spite of a low metallicity, we would suggest that the first effect is the more important one for the bulge stars.

Finally, we note that the LPVs' decrease in numbers with latitude (third column of Table 12) is comparable to that for the latest M giants (Blanco 1988; Terndrup 1988). We will return to a discussion of the distribution of the various stellar components of the bulge below.

VI. BULGE *IRAS* SOURCES

In this section we present the results of a search for *IRAS* sources in the fields surveyed for M giants. Results of more extensive searches at two latitudes in the bulge by Glass (1986) and by Whitelock, Feast, and Catchpole (1986) are compared with our findings. Finally, characteristics of the dust shells around the *IRAS* sources are examined and compared with observations of M31.

a) *Identification of IRAS Sources*

A search was made of the *IRAS* Point Source Catalog (1985) for sources within and close to the boundaries of the grism fields surveyed for this paper. Criteria for identification and problems of crowding and source confusion are discussed in FW. Identifications with M giants observed in the near-infrared are indicated in Tables 2–6. Most of these identifications are with LPVs. The remainder appear to be normal, nonvariable M giants detected by *IRAS* only because they are bright. The *IRAS* sources found within the grism fields are briefly discussed below.

i) *The* $-3°$ *Field*

The small area searched for M giants made it unlikely that any *IRAS* sources would be found here. One source, IRAS 17560−2916, lies just outside the area searched and is included in Glass's (1986) survey of the Sgr I field.

ii) *The* $-6°$ *Field*

The *IRAS* sources found in this field have colors similar to the those found in Baade's Window (FW).

18064−3154.—A faint source close to star 85 (Table 3), a blue, faint giant that is unlikely to be associated with the *IRAS* source.

18065−3152.—Although close to stars 89 and 90 (not observed) and to star 91 (Table 3), this source is probably not a star, since it was detected only at 60 and 100 μm, with the 100 μm flux being 7 times greater than that at 60 μm.

18066−3144.—The bright *IRAS* source detected only at 12 and 25 μm is probably associated with star 188, a visually bright M5–M6 giant we did not observe. The *IRAS* colors are normal for an M giant.

18069−3153.—Detected only at 12 and 25 μm, with a flux ratio typical of a cool star. No nearby M star or other visually bright object.

18069−3156.—Detected only at 60 μm; no obvious visual counterpart.

18070−3138.—Identified with star 235, the reddest star reported on in this paper. The *IRAS* fluxes are consistent with the presence of a dust shell.

18075−3137.—This source is on the edge of the grism field and would not have been included in the survey.

iii) *The* $-8°$ *Field*

All four of the *IRAS* sources within the grism field can be identified with M giants listed in Table 4 and all are LPVs. Three were identified by Plaut (1971), while the fourth is classified as an LPV on the basis of its near-infrared colors.

18144−3249.—(star 8-81), *18145−3255* (star 8-86), *18154−3254* (star 8-29).—These three sources were detected only at 12 μm by *IRAS*. Their fluxes at 12 μm are consistent with the observed 10 μm fluxes (Table 4) and are indicative of a small excess.

18150−3255.—This was detected at 12 and 25 μm and is identified with star 8-43. It does not appear to have a significantly bigger infrared excess than the other three sources found in this window; it is just brighter overall, accounting for its being detected at 25 μm.

iv) *The* $-10°$ *Field*

No *IRAS* sources could be identified with the stars in Table 5. None of the sources in the area appear to be stars with infrared excess emission as judged from their *IRAS* fluxes.

18238−3404.—Detected only at 12 μm, it corresponds to SAO 210168.

18243−3351.—Detected only at 100 μm; there are no stars near the *IRAS* position.

18255−3331.—This is probably SAO 210209.

v) *The* $-12°$ *Field*

Two *IRAS* sources are identified with M giants in Table 6. There are a few other sources within the search area, but none appear to be stars with excess emission.

18337−3434.—Detected only at 12 μm, it appears to correspond to SAO 210368.

18348−3424.—This is associated with star 12-1 in Table 6. Since it is one of the brightest stars found in any of the bulge fields, it is possibly a foreground giant and may have a mild infrared excess.

18349−3421.—Detected only at 12 and 25 μm with normal flux ratios for a late-type star, it lies close to a visually bright star just outside of the search area.

18350−3508.—Detected only at 12 μm, this source probably corresponds to an M5–M6 giant not observed in the near-infrared.

18354−3426.—Detected only at 12 and 25 μm, it is identified with star 12-17 in Table 6. One of the reddest stars in this field, it has previously been classified as an LPV. The *IRAS* fluxes are indicative of a mild infrared excess.

18357−3459.—Detected only at 12 μm, it lies close to a visually bright star in the survey region.

b) *The Results of Glass and of Whitelock, Feast, and Catchpole*

The three main conclusions concerning *IRAS* sources discussed by FW are strengthened by the data presented here: First, there is no evidence for any significant population of visually undetected luminous stars in the bulge. Second, collectively the *IRAS* sources contribute less than 5% to the integrated bolometric luminosity of the bulge and less than 10% to the luminosity at 10 μm. Finally, most of the bulge *IRAS* sources can be identified with LPVs, while the remainder are bright M giants, some of which could be foreground objects.

Extensive ground-based observations of bulge *IRAS* sources have been carried out by Glass (1986) in the Sgr I window at $b = -3°$, and by Whitelock, Feast, and Catchpole (1986, hereafter WFC) in several fields centered at $b = \pm 7°$ and at $b = \pm 8°$. Of the sources examined by Glass, a couple appear to be foreground objects, several could be associated with known bulge LPVs, whereas the remainder, Glass argues, "are probably also Miras or Mira-like variables" in the bulge. However, he could find no visible counterparts for half of this latter group. Since these also have the reddest *JHKL* colors of the *IRAS* sources in his sample, Glass suggested that circumstellar dust must be responsible for the visible obscuration. All of Glass's *IRAS* sources have *JHKL* colors that overlap the bulge LPVs in Figure 12 and extend the sequence to the red. Although their infrared luminosities tend to be brighter than the mean value for the bulge LPVs we have studied, the upper bound to their brightness is not any greater than that of the LPVs in Tables 2–6 (cf. Fig. 9 of Frogel 1988*b*). We will comment on this comparison at the end of this section.

WFC argue that the *IRAS* sources they identified can be divided into two easily distinguishable groups, "namely normal, probably foreground, M giants and [second] Mira-like objects belonging, largely, to the bulge population." Their *IRAS* sources have near-infrared colors that overlap those of the sources found by Glass, although they do not extend quite as far to the red. WFC also emphasize that they find no significant differences between their *IRAS* bulge sources and local Miras.

The luminosities of the bulge LPV-*IRAS* sources found by Glass (1986) and WFC overlap the bright end of the LPV luminosity distribution determined from our work but do not extend to higher luminosities. The overlap is only with the bright end, because the *IRAS* catalog is magnitude-limited (and strongly confusion-limited in the bulge as well). The bulge LPVs identifiable with *IRAS* sources in this paper and in FW are among the brightest examples of the bulge LPVs in the near-infrared, whereas the *IRAS* fluxes for the most part are not far above the cutoff for detectability in the *IRAS* catalog. The number of *IRAS* sources identified with giants found in the grism survey is consistent with the surface density determined from WFC's work. Hence, the results of the Glass (1986) and WFC studies of bulge *IRAS* sources are consistent with and strengthen those derived from our grism surveys and near-infrared observations as enumerated in the first paragraph of this section.

c) *Dust Shell Characteristics as a Function of Latitude*

Is there a correlation between the *IRAS* colors and the near-infrared colors for LPVs, and how do these quantities depend on latitude? WFC found the $J-K$ and $K-[12]$ colors of the sources they studied to be correlated and indicative of a wide temperature range. Here we examine their data together with those of Glass (1986) in order to investigate latitude-dependent effects. Frogel and Elias (1988) have pointed out that differences in the physical characteristics of two groups of LPVs, such as luminosity, pulsation characteristics, and metallicity, will be reflected in differing ratios of hot and cold dust for the two groups. One way to measure this ratio is to consider the $K-L$ color as indicative of hot dust and the *IRAS* value for $F_\nu(12)/F_\nu(25)$ as a measure of cold dust. We have taken values for this latter quantity from Table 1 of WFC and from the *IRAS* catalog for the sources in Glass. There is an obvious gap in the $(K-L)_0$ distribution of their sources at a value of about 0.5 (Fig. 10 of Frogel 1988*b*); we interpret this to be the demarcation between LPVs and ordinary M giants and consider only stars redder than the gap. Figure 14 shows the relation between these two quantities. The least-squares regression line was calculated excluding the outlier at $(K-L)_0 \approx 3$. The mean absolute deviation (Press *et al.* 1986) in the log of the flux ratio of the points in Figure 14 is 0.085, consistent with the uncertainties and nonsimultaneity of the *IRAS* and near-infrared data and variability of a few tenths of a magnitude in $(K-L)_0$.

The two samples in Figure 14 have systematically different deviations from the regression line. For Glass's low-latitude sample the mean value of the residual in log $[F_\nu(12)/F_\nu(25)]$ from the line is -0.035, with a 1 σ dispersion of 0.009. The corresponding values for the WFC sample at the higher latitude are $+0.031$ and 0.017. This difference indicates a relatively larger amount of cool dust around the lower latitude LPVs in the bulge. Since the luminosities of the two samples do not differ, following Frogel and Elias (1988), we attribute the

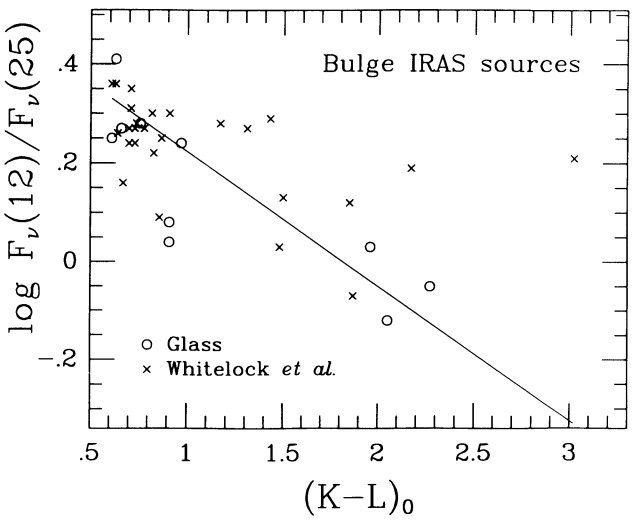

FIG. 14.—Ratio of the *IRAS* fluxes $F_\nu(12)/F_\nu(25)$ as a function of $(K-L)_0$ for bulge *IRAS* sources with $(K-L)_0 \geq 0.5$ found by Glass (1986) and Whitelock, Feast, and Catchpole (1986) and classified by them as LPVs. The least-squares regression line is shown.

difference in dust properties to metallicity and pulsation effects. High metallicity will, for equal mass-loss rates, result in more dust being expelled into a circumstellar shell than for a low-metallicity star. A higher mass-loss rate or greater pulsation amplitude, or both, in the higher metallicity stars will result in a more extended dust shell with subsequently more material at cooler temperatures. Hence detection by *IRAS* at 25 μm will have been easier, since there will be relatively more dust in cooler regions farther out from the star.

As part of a separate project, we calculated (in 1985) with the facilities available at IPAC (the *IRAS* Processing and Analysis Center) the mean value of the 12 to 25 μm flux ratio for stellar *IRAS* sources in several fields between 1° and 4° on a side. The fields were chosen to cover a range in Galactic latitude at longitudes of 0°, 180°, and 270°. In order to obtain first a list of candidate sources, the fields chosen were co-added from the *IRAS* Working Survey Data Base. Sources were then extracted with criteria meant to minimize differences that could arise in the data themselves as a result of the wide relative range in Galactic latitude. Table 13 presents the calculated mean flux ratios for the fields. The number of sources that went into calculating the ratio is given in parentheses after each entry. Two results are clear from Table 13. At 0° longitude, the lowest latitude sources have a cooler 12 to 25 μm energy distribution than higher latitude sources. This confirms the result based on Figure 14. Second, this cooler energy distribution is not seen in sources at equal latitude but at different longitudes. Thus, taken as a group the *IRAS* bulge sources have distinct characteristics. Habing *et al.* (1985) reached a similar conclusion, although they could not examine the latitude distribution, since they averaged source properties over rectangular areas 20° on a side.

d) Comparison with M31

In Baade's window half of the total 10 μm emission is "excess," i.e., cannot be attributed to normal photospheric emission from the stars that are present (FW). This is the same relative amount of excess emission observed in the central regions of typical elliptical galaxies (Impey, Wynn-Williams, and Becklin 1986) and in the bulge of M31 (Soifer *et al.* 1986). In contrast to the conclusion of these other authors, FW demonstrated that about 80% of this excess emission comes from rather ordinary M5–M7 giants with relatively weak circumstellar emission rather than from a more exotic stellar type. The stars that individually have the greatest excess at 10 μm, LPVs and *IRAS* sources, contribute the remaining 20%. *IRAS* sources by themselves contribute not more than 10% of the excess or 5% of the total 10 μm light from the Galactic bulge. From the discussion in the previous sections it is apparent that the *IRAS* sources in Baade's window are typical of those throughout the bulge, although the extent of the circumstellar emission depends on latitude. We therefore consider in somewhat more detail FW's comparison of the Galactic bulge with the integrated *IRAS* data for the bulge of M31 (Soifer *et al.* 1986; see also Frogel 1988*b*).

TABLE 13

log $[F_\nu(12)/F_\nu(25)]$[a]

	l		
b	0°	270°	180°
−3°	0.18 (89)	0.39 (12)	0.32 (111)
−4°	0.20 (221)	...	...
−7°	0.49 (8)	0.37 (31)	...
−8°	0.29 (70)	...	...
−10°	0.40 (34)	...	...
−12°	0.44 (21)	...	...
−15°	0.28 (15)	0.45 (35)	0.36 (51)
−20°	0.40 (54)	...	...
−30°	...	0.51 (5)	0.44 (20)

[a] Numbers in parentheses are numbers of sources that went into calculating the ratios.

From the analysis of Habing *et al.* (1985) we find that within 5° of the Galactic center, corresponding to the inner 3′ of M31, there are 1300 *IRAS* bulge sources that would have a total 12 μm flux of 2950 Jy. Since M31 is 100 times more distant than the Galactic center, the same number and type of sources in M31 would have a flux density of 0.3 Jy. The actual observed flux from the center of M31 within an equivalent aperture of 6′ diameter is 8.2 Jy (Table 1 of Soifer *et al.* 1986). Thus *IRAS* sources such as are seen in the Galactic bulge would contribute 4% of the total 12 μm light from M31, the same fraction as for the Galaxy. Although such close quantitative agreement is probably fortuitous, qualitatively the contributions of *IRAS* sources to the integrated 10 μm light of the Milky Way and M31 are certainly consistent with one another and lend credence to the conclusion that *IRAS sources contribute only a minor fraction of the excess emission at* 10 μm *in the bulges of normal spiral and elliptical galaxies.*

VII. INFRARED SURFACE BRIGHTNESS OF THE BULGE

Determination of the mass distribution within a kiloparsec of the center of the Galaxy is necessary for understanding the dynamics and rotation curve of the Galaxy as a whole (Bahcall 1986 and references therein). Progress has been made in understanding this mass distribution from optical data (Terndrup 1988; Blanco 1988; Blanco and Terndrup 1989), but little has yet been done in the infrared except for the region immediately around the Galactic center (Oort 1977; Frogel 1988*b* and references therein). In this section we examine star counts and integrated infrared surface brightness data for the six bulge fields we have studied.

a) Observed Source Counts and Surface Brightness Distribution

Table 14 presents six measures of the structure of the bulge along the minor axis. To facilitate comparison between number counts of objects and observed surface brightness values, we normalize the number counts by taking 2.5 log N and then adding a constant so that this quantity will equal the K surface brightness determined from the measurements of the M giants in Baade's window. Column (2) is calculated from Habing's (1986) parameterization—$N(r) = N_0 \exp(17.2 - 8.5r^{1/4})$—of counts of 12 μm *IRAS* bulge sources. Column (3) gives the normalized counts based on the distribution of LPVs from Table 12. Column (4) is derived from the sum of all M giants found in each field (from Table 7) normalized by the field sizes given in Table 8. Column (5) is the integrated 2.2 μm light measured from balloons and is discussed in more detail in the next section.

Column (6) of Table 14 is the integrated K-magnitude of the M giants in each field from Table 8 normalized to the size of one grism field. The radial dependence of this quantity will not necessarily be identical to that of the counts of the same M giants. One reason is that although the M1–M2 giants are the most numerous class of M stars in each field, they are the most

TABLE 14

SURFACE BRIGHTNESS AND SURFACE DENSITY DISTRIBUTION

Field (1)	*IRAS* (mag) (2)	LPVs (mag) (3)	N(M2–M9) (mag) (4)	K(map) (mag) (5)	K(M2–M9) (mag) (6)	V_0 (mag) (7)	$(V-I)_0$ (8)
−3°	0.21	0.68	1.00	−0.45	0.79	...	...
−4°	1.03	1.03	1.03	0.00	1.03	18.7	1.1
−6°	2.51	2.29	2.64	0.95	2.29	19.5	1.0
−8°	3.58	1.65	3.37	1.85	2.92	20.7	0.9
−10°	4.48	>4.	4.72	3.05	4.71	21.3	0.9
−12°	5.23	4.59	4.92	...	4.13	...	...
R_e(kpc)	0.08	0.19	0.15	0.21	0.23	0.23	...
σ	±0.008	±0.05	±0.013	±0.020	±0.033	±0.023	...
$n(R/R)^{-n}$	3.39	2.66	2.84	2.63	2.58	2.54	...

difficult to pick out and classify with the grism technique because of the weakness of the absorption bands used for classification (Blanco 1986). However, because of their relative faintness in the infrared (FW), a large uncertainty in their numbers translates into a small uncertainty in the integrated K-magnitude of all of the M giants. A second reason for a difference between the number counts and K surface brightness distribution of M giants is the presence of foreground giants in the fields. Since their relative number increases with increasing latitude (Terndrup 1988) and they will tend to be among the brightest stars observed, they will have a bigger influence on the K surface brightness than on the M giant counts. We consider these effects to be less serious for the K light than for the M giant counts, so that the former probably gives a more accurate picture of the bulge.[7] Finally, we have the surface brightness in V and the $V-I$ colors as determined by Terndrup (1988) from his CCD frames. These values, given in columns (7) and (8), respectively, of Table 14, have been corrected for the estimated contribution from disk stars as described by Terndrup.

b) Surface Brightness Derived from Balloon Data

A number of attempts have been made to map the central part of the Galaxy at 2.4 μm from balloon-borne telescopes. The work of Okuda *et al.* (1977), Ito, Matsumoto, and Uyama (1977), Oda *et al.* (1979), and Hiromoto *et al.* (1984) revealed the overall shape of the inner bulge of the Galaxy and of the disk for several degrees on either side of the center. Significant differences exist in the absolute flux calibrations of the various maps (Frogel 1988*b*). Matsumoto *et al.*'s (1982) map covers all but the outermost of the fields studied by us and also agrees in flux with that of Hiromoto *et al.* (1984); it will be used here in comparison with other estimates of the dependence of surface brightness on Galactic latitude.

Matsumoto *et al.*'s map was constructed with a 0°.5 beam size, only slightly bigger than the diameter of one grism field, so that the average surface brightnesses of the two should be directly comparable. For the comparison two small corrections, both of order +0.1 mag, were applied to the surface brightness values read from their maps at the latitudes of the bulge fields: to transform their values from 2.4 μm to 2.2 μm and to allow for the fact that their standard star (presumably α Sco) has a considerably stronger 2.29 μm CO band than the standards we used. Column (5) of Table 14 lists the 2.4 μm surface brightness values as read from the map and as converted to a reddening-corrected, integrated K-magnitude over an entire grism field at the appropriate latitude.

K-magnitudes from the balloon maps are expected to be brighter at each latitude than the integrated magnitudes derived from M giant observations, since the latter are sampling a limited part of the population whereas the balloon data are truly integrated values. The differences between the two sets of data can be a useful test of stellar population models. The K light of the M giants should be about 50% of the total K light in any given field (FW; Frogel 1988*a*, *b*). Table 14 shows that for each field the K light of the M giants is about 30% of the total K light as given by the balloon data. The difference does not appear to depend on latitude. In view of the uncertainties in the data and the models, we regard the agreement as quite encouraging. In fact, if Oda *et al.*'s (1979) balloon data and their flux scale were used, the observed difference between the two sets of K-magnitudes at each latitude would be quite close to 50%, the value predicted by the models.

c) Fits to the Surface Density and Surface Brightness Distributions

For each of the distributions of surface brightness or surface density in Table 14 an effective radius R_e can be determined by fitting the data to a de Vaucouleurs law of the form

$$\mu - \mu_e = 8.32[(R/R_e)^{1/4} - 1] .$$

Values for R_e so derived, together with their standard errors, are given near the bottom of the table. The confidence level of the fits is typically at the 98% level or higher. The distributions are equally well fitted by a power law of the form

$$\mu \propto (R/R_0)^{-n} .$$

The values of n are given on the last line of Table 14. The standard errors in the values of n are of the same relative size as the standard errors in the R_e values. Each point was weighted equally in both solutions, even though the points at the extrema are relatively uncertain.

The R_e values in Table 14 are a factor of 10 or more less than that used by de Vaucouleurs and Pence (1978) to fit their BV photometry exterior to 10°. All of these values are considerably less than the radius of the innermost data point. Blanco (1988; see also Blanco and Blanco 1986), Terndrup (1988), and Blanco and Terndrup (1989) have also concluded that the inner bulge

[7] Systematic errors in the number counts are essentially eliminated if one rigorously excludes the earliest type M giants from consideration. This is the approach taken by Blanco and Blanco (1986) and Blanco (1988).

has a steep density gradient on the basis of M star counts and CCD photometry. The new data presented in this paper show that the steep decline is present at all wavelengths and for several samples of objects.

IRAS sources exhibit a significantly steeper decline than do more general measures of the stellar population, such as the K light or the optical photometry.[8] This would be expected in the presence of a metallicity gradient, since the bulge *IRAS* sources are mostly associated with the reddest stars (FW; Glass 1986; WFC), which, in turn, will be heavily weighted toward the metal-rich end of the metallicity distribution. If we were to isolate the M7–M9 giants and derive their surface density as we did for all M giants, we would find $R_e = 0.10 \pm 0.016$, in agreement with the *IRAS* source distribution. This result parallels Blanco's (1988) finding that the later the spectral group examined, the steeper the falloff. As he noted, this too is consistent with a metallicity gradient in the bulge. The data on the LPVs are too sparse to say whether their surface density distribution more closely resembles that of the population as a whole or that of the very latest objects. A more complete survey for LPVs would give some indication of the relative metallicity of their parent population.

While the *differences* in the distributions of different samples of objects can be attributed to a metallicity gradient in the bulge, the *steepness* of the K and V light distribution relative to that derived by de Vaucouleurs and Pence (1978) cannot, because both the K and V light are sampling all metallicities—the V light because it is an integrated measure over entire CCD frames and comes primarily from all giants earlier than type M, from subgiants, and from evolving dwarfs. A simple stellar synthesis model for the stars in Baade's window (Frogel 1988*a*, *b*) shows that the K light from the M2–M9 giants is in fact sampling $\sim 50\%$ of the total light at K and encompasses essentially all stars brighter than $M_{\rm vol} = -1.2$ (FW), so that metal-poor stars should be represented in their correct relative number. Hence, as concluded by Terndrup (1988) and Blanco (1988) on the basis of optical data alone, the steep decline in the surface densities that measure the stellar content of the bulge as a whole cannot be attributed to metallicity.

Since metal-poor stars make up only a small fraction of the total population of the bulge (Rich 1988; Whitford and Rich 1983), the data in Table 14 will be little influenced by their presence. Yet it would be interesting to know whether radial distribution differs significantly from those of the objects in Table 14. In other words, does the bulge consist of a dominant metal-rich population superposed on a relatively metal-poor one with a spatial distribution that more closely resembles that derived by de Vaucouleurs and Pence (1978)? RR Lyrae variables should be a reasonable probe of the metal-poor component. In his Figure 3*a* Saha (1985) plots the space density for RR Lyrae stars as derived from several different surveys. For log R between 0 and 1 an eye fit to the data in this figure indicates that $\rho \propto R^{-2.25}$, or surface density is $\propto R^{-1.25}$, considerably flatter than any of the other distributions. (Note that beyond 1 kpc the decrease in density of the RR Lyrae stars becomes much steeper.) Unfortunately, this only sets a lower limit on the value of n, since, for the metallicity ranges we expect in the bulge, the relative number of RR Lyrae stars at a given [Fe/H] will decline sharply with increasing [Fe/H] because the stubbly red horizontal branch of a metal-rich population will not touch the RR Lyrae instability strip. What we need to know is the metallicity distribution itself as a function of latitude.

[8] As pointed out in Frogel (1988*b*), the fact that our value of R_e for the *IRAS* sources is so much less than the 0.6 kpc quoted by Habing *et al.* (1985) is of no significance, since their value was chosen *arbitrarily* rather than derived from the data (G. Neugebauer 1987, private communication).

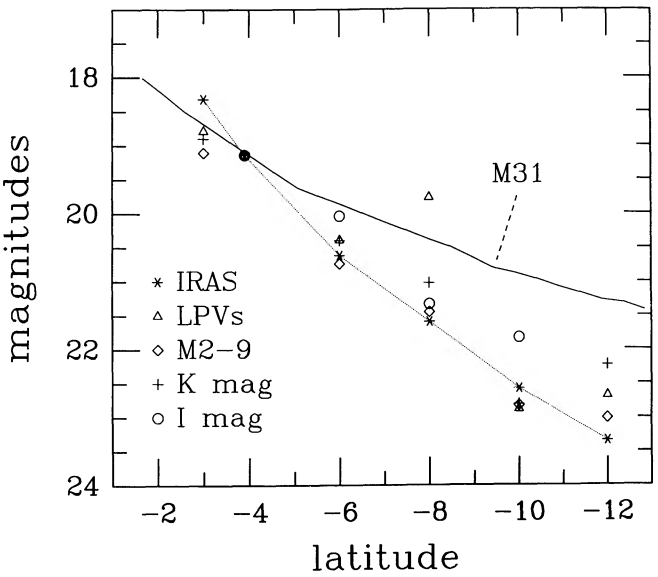

FIG. 15.—M31 minor-axis surface brightness (*solid line*; Hoessel and Melnick 1980) is compared with five measures of the radial variation of surface brightness in the Galactic bulge (Table 14). The first three of these are based on number counts, while the last two are based on photometry. All measures have been normalized at a latitude corresponding to Baade's window. The *IRAS* points are connected with a thin dotted line.

d) Comparison with Other Galaxies

Is the steep light gradient observed in the bulge between 0.4 and 1.5 kpc from the center (Table 14) typical for spiral galaxies? First we compare the bulge data with surface photometry for M31 from Hoessel and Melnick (1980). Figure 15 displays surface brightness data along M31's minor axis in the G band from their Table 2. The horizontal scale is set with the assumption that M31 is 100 times more distant than the Galactic bulge. Five of the data sets from Table 14 are plotted after normalization at $-3.^\circ 9$. Although there is considerable scatter, all of the Galactic data sets lie consistently above the M31 curve; the data for the Galactic bulge indicate a much steeper falloff with radius of surface brightness or density than is seen in M31. If the M31 data were further scaled to take into account the fact that the bulge is bigger, this conclusion would not change.

Next we compare the data in Table 14 with those for the galaxies published by Kent (1986, 1987). For 22 Sb, Sbc, and Sc galaxies from Kent closer than 30 Mpc, the differences in surface brightness between minor-axis radial distances equivalent to 3° and 12° at 7 kpc in the Galactic bulge were computed. The distribution of these values is illustrated in Figure 16. These differences range between 1.0 and 2.8 mag. The two greatest values are in NGC 4605, an Sc galaxy, and NGC 5033, an Sbc. However, almost none of the galaxies in Kent's sample is viewed edge-on. Thus at 1.5 kpc from their centers there will be a significant disk contribution to the minor-axis light profile. Blanco and Terndrup (1989) have constructed a model for the Galaxy based on optical data that incorporates a disk

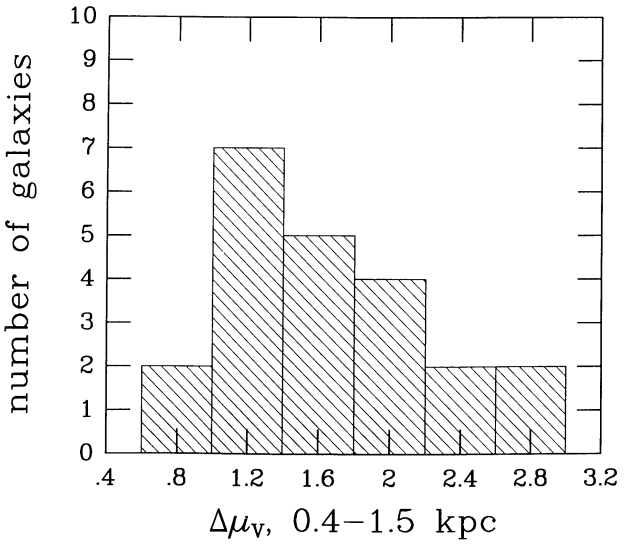

FIG. 16.—Distribution of the difference in surface brightness, in magnitudes, between radial distances equivalent to $-3°$ and $-12°$ in our Galaxy, shown for Sb–Sc galaxies, from Kent (1986, 1987).

and a sharply peaked bulge. We have shown in Table 14 that infrared and optical scale lengths for the bulge are similar; in fact the bulge scale length derived by Blanco and Terndrup is nearly the same as that found here from the M giants. From their model we calculate that the change in magnitudes in a face-on view of the Galaxy from 0.4 to 1.5 kpc would be 2.4 mag. Thus the Milky Way's bulge is similar to only the most steeply concentrated bulges in Kent's sample (see Fig. 16).

To verify the validity of the comparison with Kent's (1986, 1987) data, we looked at three potential problems. First, we could find no significant difference in the distribution illustrated in Figure 16 between near galaxies and distant ones. Galaxies from Kent's second sample (1987) are generally much closer than those in his first sample (Kent 1986). Second, we found no correlation between the values in Figure 16 and the disk ellipticity, as might be expected if the surface brightness measures in the region of interest were severely biased by the disk light contribution beyond that accounted for by Blanco and Terndrup's (1989) model. A third possibility is a reddening effect. The disks with highest ellipticity in Kent's samples do show a tendency to have smaller values of the surface brightness differences. Since reddening should increase with decreasing radial distance and thus flatten out the true surface brightness distribution, the observed weak effect may be due to internal extinction. Frogel (1985) has found A_V values as large as 1.6 mag in the nuclear regions of 19 late-type spirals. Infrared observations of the sample of galaxies studied by Kent would show whether or not the large difference in the radial dependence of surface brightness between the Milky Way and other galaxies can be partially explained by reddening.

Although uncommon, the steep gradient in surface density observed along the minor axis of the bulge of the Milky Way is not unique. As noted by Terndrup (1988), NGC 4565 has a comparably steep falloff. Since it is viewed edge-on, a direct comparison can be made between it and the Milky Way without the need to model the disk contribution. From the data of van der Kruit and Searle (1981), we see that this galaxy has a surface density along its z-axis proportional to $z^{-3.3}$. With the appropriate scaling, this would correspond to a difference in surface brightness of 4.8 mag between the $-3°$ and $-12°$ Galactic bulge fields, considerably greater, even, than any of the corresponding values in Table 14 for the Milky Way.

VIII. DISCUSSION AND CONCLUSIONS

a) Introduction and Background

In this paper we have presented infrared photometry for unbiased selections of M giants at five latitudes between $-3°$ and $-12°$ along the minor axis of the Galaxy; the samples are drawn from complete grism surveys for such stars. The framework in which we have interpreted these data has been laid down in the study of M giants in Baade's window (FW). Our new data are directly relevant to the three goals of bulge studies set forth in § I of this paper. They delineate a number of important physical properties of bulge stars, such as their bolometric luminosity function, color temperature, and molecular band strengths. The empirical determination of these physical properties imposes strict constraints on any evolutionary models that might be constructed for old, metal-rich stars. Secondly, the variation of these properties with latitude, their relation to [Fe/H] for bulge giants and its gradient within the bulge, and the radial dependence of the surface density of the giants define the observables that models for the evolution and chemical enrichment of the bulge of the Galaxy must try to match. Finally, insofar as the bulge of our Galaxy is representative of other spheroidal populations, these new data indicate the degree of variation in observable quantities with central distance, and at a given distance, that stellar synthesis models must be able to account for.

Optical studies of the bulge by van den Bergh and Herbst (1974) and Terndrup (1988) have yielded compelling evidence for the presence of a metallicity gradient over the range in radial distance relevant for this paper. The size of the optically determined gradient appears to be about a factor of 2 between $-4°$ and $-10°$, although the value is quite uncertain as it rests on several assumptions concerning how the optical properties of the stars, particularly their colors, will vary with [Fe/H]. Similarly compelling arguments from the spectroscopic analysis of K giants in Baade's window by Rich (1988) and Whitford and Rich (1983), as well as Terndrup's (1988) photometry, can be made for a large range in [Fe/H] at a given latitude; the size of the range, though, must also be regarded as uncertain because of the assumptions and extrapolations that go into its determination.

Some of the variation with latitude in the properties of the bulge M giants as derived from the infrared data can be understood qualitatively in the context of a metallicity gradient. Indeed, it would be easy to conclude from the infrared data alone that a metallicity gradient exists in the bulge. However, there are some aspects of the variation in these data that can be explained only in a very ad hoc way by such a gradient. In fact, if these parts of the data were considered by themselves, it is likely that one would conclude that there was no metallicity gradient. Also, as already pointed out by FW, the variation in the infrared properties *at a given latitude* is inconsistent with there being a spread in metallicity, even though the spectroscopic evidence for such a spread appears to be incontrovertible. In the remainder of this section we will attempt to pull together the various conclusions drawn from the new data and point out what we do or do not understand about the bulge M giants in particular and the bulge in general. Also, we will indicate the additional research topics we feel to be of impor-

tance if further progress is to be made toward achievement of the three goals of bulge studies.

b) Carbon Stars and the Luminosity Function of Bulge Giants

In none of the fields studied here, nor in the additional surveys of the bulge published by Blanco (1988), have any luminous carbon stars been found similar to those that exist in younger populations such as the Magellanic Clouds (e.g., Cohen *et al.* 1981). This "non-finding" is qualitatively consistent with the theory of thermally pulsing carbon star formation and evolution as reviewed by Iben and Renzini (1983) independent of recent modifications that have been made to it in an attempt to account for the observed upper and lower bounds to the luminosity at which carbon stars are found. In brief, if one starts out with a high-metallicity double shell burning giant, then a large number of thermal pulses, with subsequent dredge-up, are required to dilute the high abundance of O already in the outer layers with enough C from triple-α burning in the core to result in $N(\mathrm{C/O}) > 1.0$, a precondition for a giant to exhibit the properties of a carbon star. If the star begins its ascent of the second giant branch with a mass less than some critical value, i.e., with a great enough age for a given [Fe/H], then before enough thermal pulses will have taken place to produce $N(\mathrm{C/O}) > 1.0$ the entire outer envelope of the star will have been shed via various mass-loss processes and lost by nuclear burning at the base. Transformation into a luminous carbon star will be impossible. Clearly, this must be the situation for the bulge giants: they are too old and too metal-rich to become carbon stars.

Although the absence of luminous C stars in the bulge sets an upper limit to their mass, another observational fact sets a lower limit: the bolometric luminosity of the brightest giants. As first pointed out by Frogel and Whitford (1982) for stars in Baade's window, there are significant numbers of giants found in each of the fields studied with bolometric luminosities about 1 mag brighter than the top of the first giant branch for stars of solar metallicity. As they pointed out, this can be understood in the context of stellar interior models, since the more metal-rich a star, the slower it burns its nuclear fuel while on the main sequence. Hence, for stars of a given age, the more metal-rich one is, the greater will be its mass when it reaches the base of the first and second red giant branches. Greater mass will allow it to ascend to a higher luminosity on the second giant branch than would a star of lower metallicity. This explanation has been supported by VandenBerg and Laskarides's (1987) stellar model calculations.

The present data raise an interesting question about the presence of luminous giants in the bulge. The luminosity functions determined for the various fields are basically indistinguishable from one another. In particular, within the uncertainties, they all have the same high-luminosity cutoff. The highest latitude fields have mean metallicities a few times greater than those of the metal-rich globular clusters with LPVs. Hence, according to Frogel and Whitford's (1982) explanation, it is not surprising that the maximum AGB luminosity reached in these outer fields is comparable to or somewhat greater than the maximum seen in the metal-rich clusters. However, their explanation would predict that the cutoff luminosity should increase significantly with decreasing latitude if the mean metallicity of the $-12°$ field is a factor of 2 or more less than that of the $-3°$ one. This is not seen.

It would be possible to account for the constancy in cutoff luminosity at different latitudes if the higher metallicity stars also have higher mass-loss rates (MLRs). Then their advantage over lower metallicity stars in starting out with a higher mass at the base of the giant branch is literally evaporated. Evidence for MLRs of LPVs considerably in excess of that predicted by the Reimers formula comes from observations (Frogel and Elias 1988) and theoretical calculations (Wood 1979; Bedijn 1988; Bowen 1988), although the very high rates derived by Frogel and Elias have been questioned (Renzini and Fusi-Pecci 1988). The theoretical calculations show that the shocks generated by the pulsations of an LPV result in a greatly extended atmosphere and more dust formation. It is radiation pressure on the dust that results in the high MLRs. These calculations also show that the MLR rapidly increases as the stars evolve up the AGB. This rapid increase does not require a phase transition in the pulsating stars. We speculate that the lifetimes may become so short after a while that the chances of seeing a star with a dust shell much thicker than those that are seen in the bulge is slight. In the same speculative vein, we ask whether the Frogel and Whitford (1982) explanation ceases to be operative for $M_{\mathrm{bol}} \leq -4.2$, independent of metallicity, for reasons connected with evolution on the upper AGB.

c) Metallicity Effects

Since the location of giants from globular clusters, the solar neighborhood, and Baade's window—a sequence of increasing mean metallicity—shifts systematically in the $(J-H, H-K)$-plane, it seemed reasonable to attribute the shift to the effects of metallicity (FW) on the colors. It is important to emphasize that the character of this shift implies that it must be due primarily to causes other than a shift of the giant branch to cooler temperatures as [Fe/H] is increased, since while $H-K$ gets progressively redder, $J-H$ gets bluer. FW argued the H_2O might be a prime candidate for the blanketing agent. The new data have revealed, though, that the situation must be considerably more complex as the relative displacement of stars from different windows in the JHK plane is nearly independent of H_2O. The interplay of decreasing temperature and increasing molecular blanketing must be quite complex. Giants from nearly all globular clusters studied in the near-infrared (Frogel, Persson, and Cohen 1983) with a range in abundance of nearly a factor of 100 have essentially identical locations in the JHK plane—all are shifted by about the same amount relative to the local field giant line. Similarly for M giants within a given bulge field: their scatter is not significantly greater than that expected from measuring uncertainties alone. There is no evidence for the large range in metallicity found spectroscopically by Rich (1988) or photometrically by Terndrup (1988). In view of the fact that the globular cluster giants share this behavior, we do not regard it as contradicting or challenging the metallicity spread found with other techniques. It must be related to the fact that the giant branches of the bulge fields are markedly blue for their high metallicity.

A more troubling result is the lack of scatter in the CO index within a given field. Again we find that the observed scatter is consistent with that expected from observational uncertainties by themselves. For the case of CO it is well established that this is a sensitive metallicity indicator in globular cluster, open cluster, and other types of giants. It is possible that saturation effects set in above a certain metallicity and prevent the observed index from getting any stronger; recall that the reason cool supergiants have much higher values of the CO index than ordinary giants is that the greater microturbulent velocities in the atmospheres of the former stars remove some

of the effects of saturation (Frogel 1971). On the other hand, the field-to-field spread in the CO index is significant and comparable to what would be expected from the metallicity gradient. In fact, the field-to-field spread in the *JHK* plane is also large. We note that if a correction were applied to $J-K$ to take into account the fact that the low-latitude fields are too blue with respect to the high-latitude, lower metallicity ones, the difference in the mean CO indices between the fields, measured at constant $J-K$, would be reduced somewhat. It is possible that the CO index is too crude a measure of the true CO band strength. A program of spectroscopically measuring this band in a sample of bulge giants from the different fields would be worthwhile. Finally, we note that although the overall dispersion in both CO and $H-K$ within a field is of size comparable to the measuring uncertainties, the correlation between the individual dispersions is statistically significant and in the same sense that these two quantities change in going from field to field.

All of this seemingly contradictory behavior of the infrared colors, magnitudes, and indices emphasizes the need to achieve new insight into the causes and effects of molecular blanketing in high-metallicity stars. Such blanketing may be great enough to seriously influence the stars' evolutionary tracks and the rate at which they recycle enriched gas into the interstellar medium. Since there are blanketing effects in optical color-magnitude diagrams as well (e.g., Terndrup 1988), account must be taken of them if evolutionary tracks are to be used to predict colors of metal-rich populations at large look-back times such as those that would be found in elliptical galaxies.

d) LPVs, IRAS Sources, and Mass Loss

Now we turn to the LPVs and the *IRAS* sources. It is likely that most of the bulge M giants go through an LPV phase just before they end their lives as giants. During this relatively brief period they dump copious amounts of matter into the interstellar medium of the bulge. If for no other reason but to learn about the nature and amount of this material, a study of the bulge LPVs would be worthwhile. Based on our present work, that of FW, and that of astronomers at the South African Astronomical Observatory (SAAO), it seems clear that most of the bulge *IRAS* sources are merely extreme examples of known LPVs, and many can in fact be identified with optical variables. While they are not any more luminous than the previously known LPVs, they have the reddest colors and longest periods of stars of this type. Nearly all of the *IRAS* sources not identified with LPVs are most likely foreground M giants and will not be considered further in this discussion. Henceforth both *IRAS* and non–*IRAS* LPVs will be referred to collectively as LPVs unless we want to single out one group or the other. At all latitudes the majority of LPVs have *JHKL* colors that lie in a tight clump close to, but distinctly separated from, the regions in the various color-color plots occupied by non–LPVs. These color-color clumps correspond to the areas occupied by globular cluster LPVs and the majority of field LPVs. The ones with more extreme *JHKL* colors define rather tight sequences in the $(J-H, H-K)$- and the $(J-K, K-L)$-plane. As concluded by FW, these sequences represent an increasing contribution from warm ($\sim$700–1000 K) circumstellar dust to the near-infrared energy distribution.

LPVs with the most extreme *JHKL* colors are relatively less frequent in the higher latitude fields. From our work and particularly from the more extensive studies carried out by the astronomers at the SAAO, it also appears that the percentage of optically obscured *IRAS* bulge LPVs is greatest in the lowest latitude fields. Together, these results suggest that the amount of circumstellar dust is a decreasing function of latitude. This conclusion is consistent with a statistical study of several hundred *IRAS* bulge sources that revealed an increase in the 12 to 25 μm color temperature with increasing latitude. As the amount of dust goes down, the shell becomes less extensive; what is left is relatively close to the central star and hence hotter.

The latitude variation of the dust shell properties of the LPVs is naturally explained by the presence of a metallicity gradient in the bulge. There are several effects operating. First of all, dust is expected to make up a higher percentage of expelled material in a metal-rich object than in a metal-poor one. Second, there are a number of phenomena believed to be responsible for mass loss in an LPV that are themselves metallicity-sensitive. One of these is the amplitude of the pulsation itself; another is the momentum transfer to the gas from the stellar radiation field via the dust—less dust, less momentum transfer. While there is little doubt that the dust-to-gas ratio will vary in a way that follows the metallicity gradient, there is some question about the role of metallicity in the mass-loss process itself. Frogel and Elias (1988) have reached the rather controversial conclusion that the *total* mass-loss rate in globular cluster LPVs is no less than that in field LPVs of considerably greater metal abundance. A more detailed study of the bulge LPVs and their dust shells would be a worthwhile undertaking both for stellar evolution theory and for understanding the recycling process of material in or near the center of the Galaxy.

Aside from interest in bulge LPVs qua LPVs, the fact that their mean bolometric luminosity is comparable to that of globular cluster LPVs implies that these luminosities cannot be used as evidence for the argument that there is a component to the bulge population significantly younger than globular clusters.

e) Structure of the Bulge

The final topic we considered in this paper is the surface density gradient within the bulge. If a power-law dependence is assumed, we have shown that a number of independent estimates of this gradient yield values for the exponent of between 2.5 and 3.5. Consistent with Blanco's (1968) work, estimators drawn from the high side of the metallicity distribution, e.g., the latest M giants, LPVs, and *IRAS* sources, have a steeper falloff than do more representative samples, such as all of the M stars or the integrated V and K light. But all samples fall off considerably more rapidly than would be inferred by simple extrapolation of the de Vaucouleurs and Pence distribution determined for the Galactic spheroid exterior to 10° from the center. This comparison and its implications are discussed in detail by Blanco and Terndrup (1989). Here we merely point out the importance of carrying out surface density studies interior to the Sgr I window to ascertain the structure of the inner bulge. In view of the fact that the density distribution we have found is also steeper than that seen in most other spiral galaxies at optical wavelengths, we have embarked on a study of a sample of Sb–Sc spirals to determine the distribution of K light within them at radii corresponding to those studied in our own Galaxy.

The close similarity of the V and K light distributions, where the K light is measured by adding up the contribution from the identified M giants alone, implies that the M stars are indeed

good tracers of the total light of stellar systems like the bulge—for example, other spiral bulges and the inner parts of spheroidal galaxies. So long as there is not a significant amount of dark matter in galactic bulges, the M stars will then be good tracers of the total mass distribution as well.

f) *Final Thoughts*

In summary, we have found considerable ambiguities in understanding colors of the bulge M giants, particularly since the colors are not uniquely related to effective temperature. Ideally, one would like an interpretation that links the physical characteristics and evolutionary state of the M giants in the bulge with those of their counterparts in the solar neighborhood and with the coolest stars in the metal-rich globular clusters. Such an interpretation may not be possible, though, until model atmosphere codes and stellar evolutionary tracks can be produced that accurately encompass the range in physical parameters that are inferred for stars in the bulge. In particular we refer to their high metallicity, old age, and cool temperature.

Aside from obvious differences in metallicity between the bulge and the disk near the Sun, what additional influences were exerted on the bulge giants by the special environment in which they formed? Given the color trends we have found among these stars and the differences between them and stars from the solar neighborhood, it appears possible that there has been a parameter aside from metallicity that has played a role in determining their present-day appearance. The same may be said about some of the differences between both of these groups and globular cluster giants. Our next two papers on the interpretation of spectrophotometric data for a subset of the bulge giants with infrared photometry should help to clarify and resolve some of the issues raised in this paper and in FW. Finally, we have mentioned the value of studying the region interior to the lowest latitude field we have examined. Of equal interest would be to observe outward from $-12°$ (the old halo population) and see whether a smooth transition to the properties displayed by the metal-poor globular cluster giants is found. One should extend such observations in longitude as well, in case there is a connection to the more metal-rich disk globular cluster population.

We thank the CTIO Telescope Assignment Committee for awarding this research project the observing time it required over a considerable number of years. The diligence and expertise of the CTIO mountain support staff allowed us to make maximum use of our allotted time. Brooke Gregory and Roger Smith made major contributions to the excellence of the detector systems. Roger Davies made a number of useful suggestions with regard to the surface brightness and density distributions. George Helou and Perry Hacking provided considerable assistance with work on the *IRAS* data base at IPAC. J. A. F. again acknowledges the hospitality of Michael Feast and the staff at the ASSO, where a good part of the preliminary analysis for this paper was done in 1986.

REFERENCES

Aaronson, M., Frogel, J. A., and Persson, S. E. 1978, *Ap. J.*, **220**, 442.
Arp, H. C. 1965, *Ap. J.*, **141**, 45.
Bahcall, J. N. 1986, *Ann. Rev. Astr. Ap.*, **24**, 577.
Bedijn, P. J. 1988, *Astr. Ap.*, **205**, 105.
Blanco, V. M. 1986, *A.J.*, **91**, 290.
———. 1987, *A.J.*, **92**, 321.
———. 1988, *A.J.*, **95**, 1400.
Blanco, V. M., and Blanco, B. M. 1986, *Ap. Space Sci.*, **118**, 365.
Blanco, V. M., McCarthy, M. F., and Blanco, B. M. 1984, *A.J.*, **89**, 636 (BMB).
Blanco, V. M., and Terndrup, D. M. 1989, *A.J.*, **98**, 843.
Blanco, V. M., Terndrup, D. M., and Frogel, J. A. 1990, in preparation.
Bowen, G. H. 1988, *Ap. J.*, **329**, 299.
Burstein, D., and Heiles, C. 1982, *A.J.*, **87**, 1165.
Cohen, J. G., Frogel, J. A., and Persson, S. E. 1978, *Ap. J.*, **222**, 165.
Cohen, J. G., Frogel, J. A., Persson, S. E., and Elias, J. H. 1981, *Ap. J.*, **249**, 481.
de Vaucouleurs, G., and Pence, W. D. 1978, *A.J.*, **83**, 1163.
Elias, J. H., Frogel, J. A., Matthews, K., and Neugebauer, G. 1982, *A.J.*, **87**, 1029.
Feast, M. W., Robertson, B. S. C., Catchpole, R. M., Lloyd Evans, T., Glass, I. S., and Carter, B. S. 1982, *M.N.R.A.S.*, **201**, 439.
Frogel, J. A. 1971, Ph.D. thesis, California Institute of Technology.
———. 1983, *Ap. J.*, **272**, 167.
———. 1985, *Ap. J.*, **298**, 528.
———. 1988*a*, in *Towards Understanding Galaxies at Large Redshift*, ed. R. Kron and A. Renzini (Dordrecht: Reidel), 1.
———. 1988*b*, *Ann. Rev. Astr. Ap.*, **26**, 51.
Frogel, J. A., Blanco, V. M., and Whitford, A. E. 1984, in *IAU Symposium 105, Observational Tests of Stellar Evolution Theory*, ed. A. Maeder and A. Renzini (Dordrecht: Reidel), p. 571.
Frogel, J. A., Cohen, J. G., and Persson, S. E. 1983, *Ap. J.*, **275**, 773 (FCP83).
Frogel, J. A., and Elias, J. H. 1988, *Ap. J.*, **324**, 823.
Frogel, J. A., Persson, S. E., Aaronson, M., and Matthews, K. 1978, *Ap. J.*, **220**, 75 (FPAM).
Frogel, J. A., Persson, S. E., and Cohen, J. G. 1981, *Ap. J.*, **246**, 842.
———. 1983, *Ap. J. Suppl.*, **53**, 713.
Frogel, J. A., and Whitford, A. E. 1982, *Ap. J. (Letters)*, **259**, L7.
———. 1987, *Ap. J.*, **320**, 199 (FW).
Frogel, J. A., Whitford, A. E., and Rich, R. M. 1984, *A.J.*, **89**, 1536.
Glass, I. S. 1986, *M.N.R.A.S.*, **221**, 879.
Habing, H. J. 1986, in *Light on Dark Matter*, ed. F. Israel (Dordrecht: Reidel), p. 329.
Habing, H. J., Olnon, F. M., Chester, T., Gillett, F., Rowan-Robinson, M., and Neugebauer, G. 1985, *Astr. Ap.*, **152**, L1.
Harmon, R., and Gilmore, G. 1987, in *Proc. Third IRAS Conference, Comets to Cosmology*, ed. A. Lawrence (Berlin: Springer-Verlag).
Hiromoto, N., Maihara, T., Mizutani, K., Takami, H., Shibai, H., and Okuda, H. 1984, *Astr. Ap.*, **139**, 309.
Hoessel, J. G., and Melnick, J. 1980, *Astr. Ap.*, **84**, 317.
Houdashelt, M., Frogel, J. A., Cohen, J. G., and Persson, S. E. 1990, in preparation.
Iben, I., Jr., and Renzini, A. 1983, *Ann. Rev. Astr. Ap.*, **21**, 271.
Impey, C. D., Wynn-Williams, G., and Becklin, E. E. 1986, *Ap. J.*, **309**, 572.
IRAS Point Source Catalog. 1985, Joint *IRAS* Science Working Group (Washington, DC: GPO).
Ito, K., Matsumoto, T., and Uyama, K. 1977, *Nature*, **265**, 517.
Kent, S. M. 1986, *A.J.*, **91**, 1301.
———. 1987, *A.J.*, **93**, 816.
Lebofsky, M. J., and Rieke, G. H. 1987, in *AIP Conf. Proc. 155, The Galactic Center*, ed. D. C. Backer (New York: AIP), p. 79.
Matsumoto, T., Hayakawa, S. Koizumi, H., Murakami, H., Uyama, K., Yamagami, T., and Thomas, J. A. 1982, in *AIP Conf. Proc. 83, The Galactic Center*, ed. G. R. Riegler and R. D. Blandford, (New York: AIP), p. 48.
Oda, N., Maihara, T. Sugiyama, T., and Okuda, H. 1979, *Astr. Ap.*, **72**, 309.
Okuda, H., Maihara, T., Oda, N., and Sugiyama, T. 1977, *Nature*, **265**, 515.
Oort, J. H. 1977, *Ann. Rev. Astr. Ap.*, **15**, 295.
Plaut, L. 1971, *Astr. Ap. Suppl.*, **4**, 75.
Press, W. H., Flannery, B. P., Teukolsky, S. A., and Vetterling, W. T. 1986, *Numerical Recipes* (Cambridge: Cambridge University Press), p. 456.
Reid, M. J. 1989, in *IAU Symposium 136, The Center of the Galaxy*, ed. M. Morris (Dordrecht: Kluwer), p. 37.
Renzini, A., and Fusi-Pecci, F. 1988, *Ann. Rev. Astr. Ap.*, **26**, 199.
Rich, R. M. 1985, *Mem. Soc. Astr. Italiana*, **56**, 23.
———. 1988, *A.J.*, **95**, 828.
Saha, A. 1985, *Ap. J.*, **289**, 310.
Smith, G. H. 1988, *Pub. A.S.P.*, **100**, 1104.
Soifer, B. T., Rice, W. L., Mould, J. R., Gillett, F. C., Rowan-Robinson, M., and Habing, H. J. 1986, *Ap. J.*, **304**, 651.
Terndrup, D. M. 1988, *A.J.*, **96**, 884.
Terndrup, D. M., Frogel, J. A., and Whitford, A. E. 1989, *Ap. J.*, submitted (Paper III).
VandenBerg, D. A., and Laskarides, P. G. 1987, *Ap. J., Suppl.*, **64**, 103.
van den Bergh, S., and Herbst, E. 1974, *A.J.*, **79**, 603.
van der Kruit, P. C., and Searle, L. 1981, *Astr. Ap.*, **95**, 105.
Whitelock, P., Feast, M. W., and Catchpole, R. 1986, *M.N.R.A.S.*, **222**, 1 (WFC).
Whitford, A. E. 1978, *Ap. J.*, **226**, 777.

Whitford, A. E. 1985, *Pub. A.S.P.*, **97**, 205.
———. 1986, in *Spectral Evolution of Galaxies*, ed. C. Chiosi and A. Renzini (Dordrecht: Reidel), p. 157.
Whitford, A. E., and Rich, R. M. 1983, *Ap. J.*, **274**, 723.
Whitford, A. E., Terndrup, D. M., and Frogel, J. A. 1990, in preparation (Paper IV).
Winnberg, A., Baud, B., Matthews, H. E., Habing, H. J., and Olnon, F. M. 1985, *Ap. J. (Letters)*, **291**, L45.
Wood, P. R. 1979, *Ap. J.*, **227**, 220.
Wood, P. R., and Bessell, M. S. 1983, *Ap. J.*, **265**, 748.
Zinn, R. 1980, *Ap. J. Suppl.*, **42**, 19.

V. M. BLANCO and DON M. TERNDRUP: Cerro Tololo Inter-American Observatory, Casilla 603, La Serena, Chile

JAY A. FROGEL: Department of Astronomy, The Ohio State University, 174 West 18th Avenue, Columbus, OH 43210

A. E. WHITFORD: Lick Observatory, University of California at Santa Cruz, Santa Cruz, CA 95064